6-21-90 JT ①

CONTRACTOR REPORT

SAND89—7043
Unlimited Release
UC—275

Silicon Concentrator Solar Cell Development

M. A. Green, Zhao Jianhua, Wang Aihua, A. W. Blakers
University of New South Wales
Kensington, N. S. W. 2033
AUSTRALIA

Prepared by Sandia National Laboratories Albuquerque, New Mexico 87185
and Livermore, California 94550 for the United States Department of Energy
under Contract DE-AC04-76DP00789

Printed May 1990

Issued by Sandia National Laboratories, operated for the United States Department of Energy by Sandia Corporation.

Printed in the United States of America. This report has been reproduced directly from the best available copy.

Available to DOE and DOE contractors from
Office of Scientific and Technical Information
PO Box 62
Oak Ridge, TN 37831

Prices available from (615) 576-8401, FTS 626-8401

Available to the public from
National Technical Information Service
US Department of Commerce
5285 Port Royal Rd
Springfield, VA 22161

NTIS price codes
Printed copy: A03
Microfiche copy: A01

SAND--89-7043

DE90 011782

SAND89-7043
Unlimited Release
Printed May 1990

Silicon Concentrator Solar Cell Development

M.A. Green, Zhao Jianhua
Wang Aihua, A.W. Blakers
University of New South Wales
Kensington, N.S.W. 2033
Australia

Sandia Contract: 06-6885

ABSTRACT

This project involved the development and supply of 550 silicon concentrator solar cells for use in prototype point-focus concentrator modules. The cells were to have a designed illumination area of 12.5 mm by 12.5 mm and to be designed for use with prismatic covers at a geometric concentration ratio of 200X. The target efficiency of 24% was comfortably exceeded, with efficiencies as high as 25.2% reached in the designed concentration ratio range. A combined lens/cell efficiency of 20.4% was measured at Sandia using a cell supplied during this project and a point-focus Fresnel lens. Subsequently, a peak module efficiency of 20.3% was achieved at Sandia using 12 cells and lenses. This is believed to be the first photovoltaic module to surpass the 20% efficiency milestone.

ACKNOWLEDGMENTS

The authors would like to thank the other members of the Solar Photovoltaic Laboratory who contributed to this project, particularly Mike Willison and Erik Keller. We would also like to acknowledge the many contributions made by Sandia staff including those by Alex Maish (Technical Monitor), Beth Richards, Clement Chiang, David King and Paul Basore.

TABLE OF CONTENTS

SECTION 1

1. SUMMARY

1.1 Objectives

The objective of this project conducted over the period from November 1987 to October 1988 was the design and fabrication of a large number of high-efficiency module-ready silicon solar cells for use in prototype point-focus concentrator modules. A total of 300 high-efficiency cells was to be supplied with a target efficiency of 24% under a 200X geometric concentration ratio, together with a total of 250 electrically active and mechanical samples. The designed illumination area of the cell was 12.5-mm x 12.5-mm square for a cell of a total area of 18-mm x 18-mm square. The cell was to be designed for use with a prismatic cover with a grid coverage fraction dictated by the prismatic cover design.

1.2 Major Results

The target efficiency of 24% was comfortably reached with a peak efficiency of 25.2% demonstrated for the best cell measured to date after application of the prismatic covers. The peak efficiency ultimately demonstrated by cells supplied during the project may lie close to 26%, given that the cell that demonstrated the 25.2% figure was only the 16th most efficient cell supplied based on measurements prior to cover application.

For approximately 40 cells for which information before and after application of the prismatic covers was available at the time of initial report preparation (December 1988), application of the covers increased the cell power output at 190-suns concentration by an average of 13.1% compared to the average measured front grid coverage for these cells of 14.8%. (A one-sun concentration is assumed to be 1000 W/m^2). This indicates a high optical efficiency for the covers under the reasonably well-collimated light from the solar simulator. About half the difference between the above figures can be attributed to increased resistance loss in the cell due to the increased current densities in the cell after application of the covers, and about half can be attributed to optical losses due to the prismatic covers.

Testing at Sandia National Laboratories indicated a reduction in this optical efficiency for obliquely incident light within the designed acceptance angle range of the prismatic cover. This is believed to be due to the cover and adhesive thickness being larger than the design value. Despite this limitation, a combined lens/cell peak efficiency (at 800 W/m^2 and 25°C cell temperature) of 20.4% was measured at Sandia using a point-focus Fresnel lens and one of the cells supplied during the present project. Using a lower concentration ratio linear Fresnel lens and another such cell, ENTECH measured over a 20% peak lens/cell efficiency. These are believed to be the first occasions peak lens/cell efficiencies above 20% have been measured using silicon cells. Subsequently, Sandia measured a 20.3% efficiency (800W/m^2, 25°C cell temperature) from a module containing 12 lens/cell units, apparently the first photovoltaic module to surpass the 20% efficiency milestone.

SECTION 2

2. CELL DESIGN AND INITIAL RESULTS

2.1 Introduction

The initial phase of the project involved the design of the cell metallization pattern and the corresponding processing masks. Then the mask design and cell processing sequences were verified by fabricating the first batches of cells for evaluation at Sandia.

2.2 Metallization Design

Initial specifications for the cell were that it have a designed illumination area 12.5-mm x 12.5-mm square, a total area of 18-mm x 18-mm square and a 2.75-mm bus width which was to include a 2.25-mm metallization band and a 0.5-mm unmetallized border around the cell perimeter. The metallization fingers were to be designed to be consistent with the cell prismatic cover developed by Entech.

The final specifications for these fingers were that they were to be parallel on a 5-mil (127-μm) center-to-center spacing and cover 15% of the designed illumination area. This corresponds to a final finger width of 19-μm. Since silver plating was to be used to make the metallization as thick as possible and since the finger width increases during the plating, the optimum design is to have the finger width as small as possible before plating. For the present cells, a value of 4-μm was chosen for this initial width. After plating approximately 7.5-μm of silver, this finger width would broaden out to the desired final value of 19-μm with a final cross-sectional area of about 120-μm^2.

There was still a choice as to whether the fingers ran parallel to an edge of the cell or diagonally across the cell. An analysis by Paul Basore of Sandia [1] showed that both designs were equivalent in terms of finger losses. However, the former configuration was chosen since it was more consistent with the method used to apply the prismatic covers. This gave the final cell design of Figure 2.1. The busbars segments running parallel to the fingers were provided to enable adhesive thickness gauges to be mounted for use in

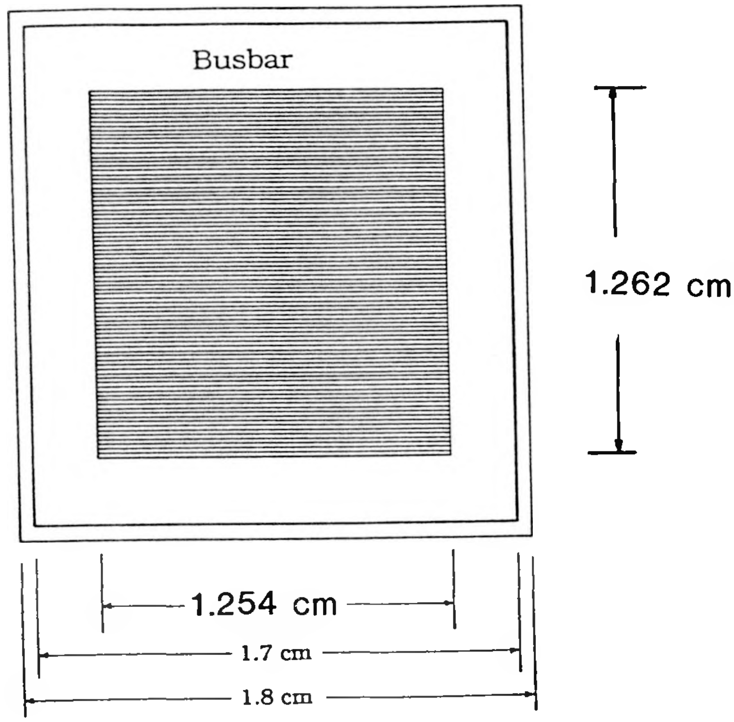

Figure 2.1: Top contact metallization design used in the present project

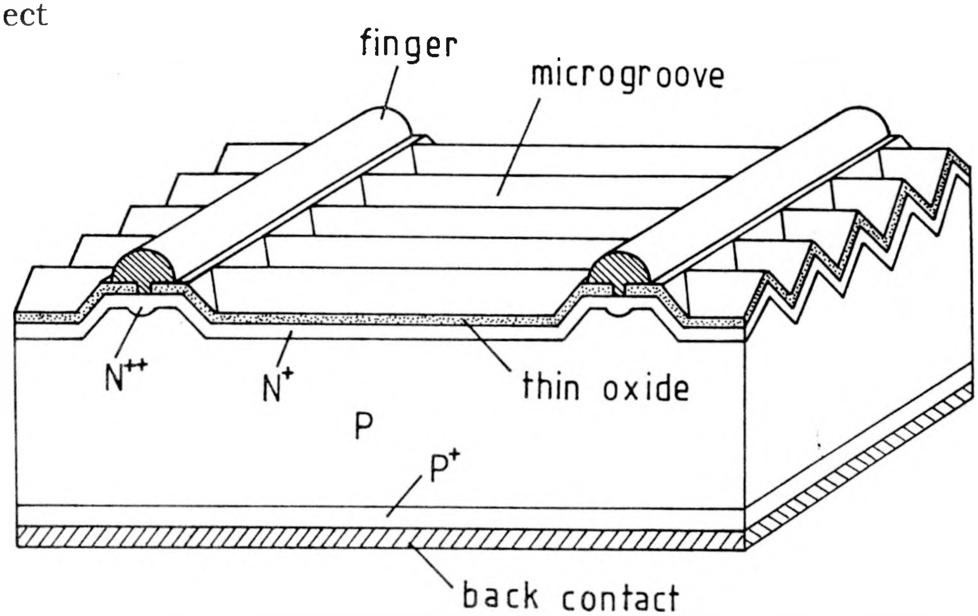

Figure 2.2: Microgrooved passivated emitter solar cell (μg PESC cell)

applying the prismatic covers. These busbars provide some additional redundancy, but otherwise do not contribute electrically to performance. Advances in prismatic cover application techniques have been made which would enable the area of these side busbars to be reduced or eliminated, reducing the area and therefore the cost of the cell.

2.3 Cell Structure

In the designed illumination area, the microgrooved passivated emitter solar cell (μg PESC) structure of Figure 2.2 as described elsewhere [2] was used. The fingers were aligned to flat regions of the cell surface as shown. The microgrooves run perpendicular to these fingers, which reduces resistance losses associated with lateral current flow in the diffused emitter of the cell. A double layer antireflection coating (ZnS/MgF_2) was vacuum evaporated onto the designed illumination area, but was masked from busbar regions by a metal mask during the evaporation step in order to facilitate interconnect soldering to be busbar.

Figure 2.3 shows micrographs of the cell structure prepared at Sandia National Laboratories. The busbars of the cell sit on relatively thick oxide pads as shown in Figure 2.4 isolating them from the silicon surface. The effects of imperfect isolation are described in Section 4.2.

2.4 Cell Processing

An outline of the cell processing sequence used in this work is given in Table 2.1.

The initial processing steps produced the microgrooving of the designed illumination area of the cell. This was followed by the heavy diffusion of the areas underlying the contact strip for the finger metallization and a second lighter diffusion of the entire designed illumination area. This was then followed by the growth and definition of the oxide pads for the busbars. Aluminum (Al) was then evaporated on the rear of the cell and alloyed, during which the thin passivating oxide grew on the top surface of the cell. This oxide was patterned, and a thin titanium, palladium, silver (Ti/Pd/Ag) multilayer was deposited on the top surface and was

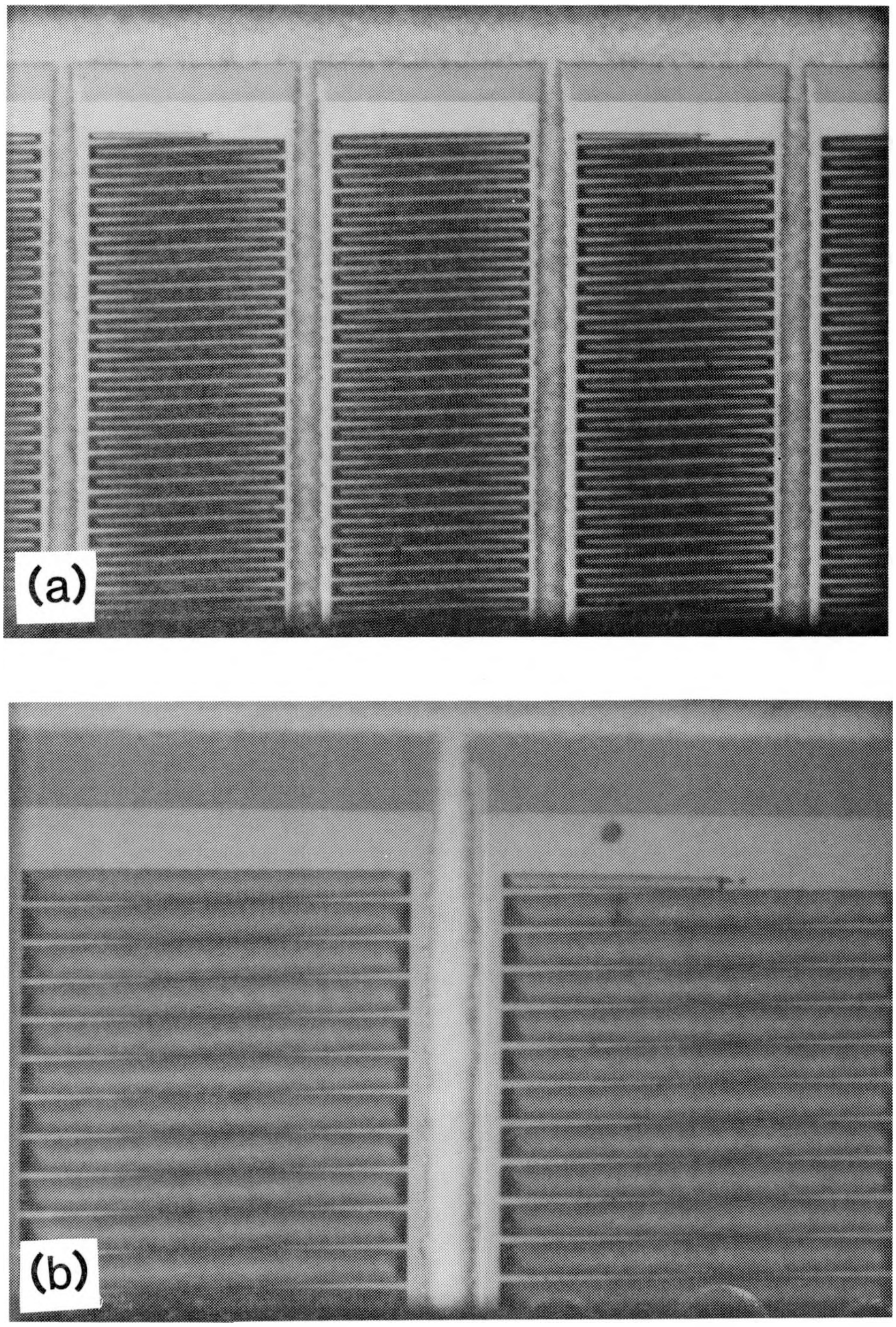

Figure 2.3: Micrographs of the surface of experimental cells showing the region where fingers contact the cell busbar. Apparent in (a) are the flat regions on which the fingers are located (center-to-center spacing of 127-μm) while (b) shows flat regions at the top of the microgrooves (center-to-center spacing of 10-μm) which taper in this specimen.

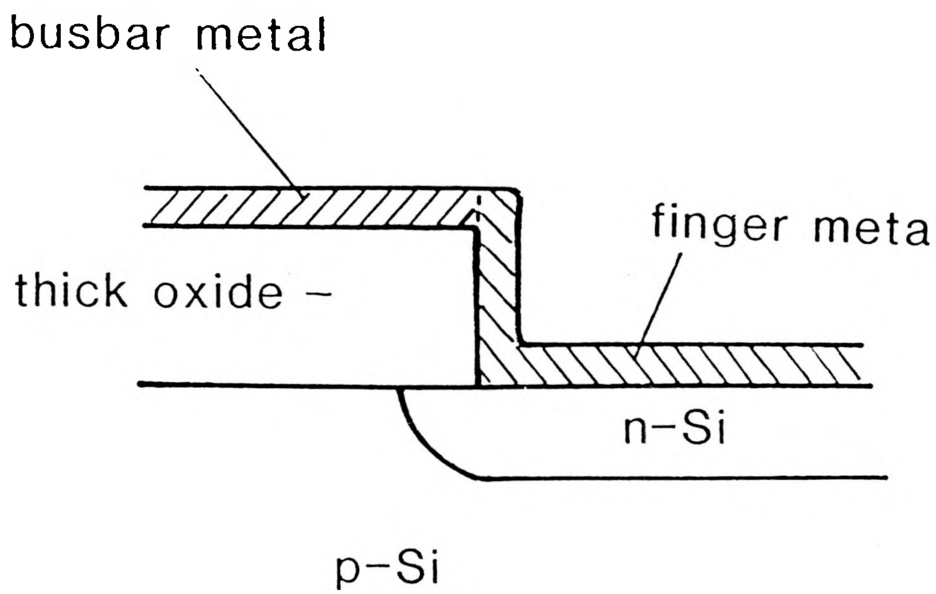

Figure 2.4: Busbar isolation using oxide pads

Table 2.1: Outline of prismatic cover cell processing sequence.

STEP	PARAMETERS
1. Wafer Selection	0.1 or 0.2 Ω-cm (100), FZ, p-Si, 280 μm thick, 5.08 cm diameter wafers
2. Oxide Growth and Patterning	950°C, wet N_2, 1000 Å SiO_2 (microgrooves on active area)
3. Microgrooving	8% NaOH, 70°C, 10 min.
4. Oxide Removal	Buffered HF
5. Oxide Growth and Patterning	1000°C, wet N_2, 5000 Å SiO_2 (n^{++} region)
6. Phosphorus Diffusion	Solid source, 950°C, 15 Ω/square
7. Deglaze	HF:H_2O = 1:15
8. Oxide Growth and Patterning	950°C, wet N_2 (planar emitter)
9. Phosphorus Diffusion	Solid source, 850°C, 180 Ω/square
10. Deglaze	HF:H_2O = 1:15
11. Rear Al deposition	Vacuum evaporation, 1 μm
12. Al Alloy and Thin Oxide Growth	950°C, O_2 (30 min.), N_2 (3 hr.), ~100 Å SiO_2
13. Thin Oxide Patterning	Metallization
14. Top Contact Metal Deposition and Lift-off	Ti/Pd (600/600 Å)
15. Rear Contact Metal Deposition	Al/Ti/Pd/Ag (0.5/0.1/0.1/6 μm)
16. Ag Plating	8 μm, top contact
17. Sinter	Forming gas, 375°C
18. AR Coating	500Å ZnS, 1100Å MgF_2

then patterned using a "lift-off" approach. A four-layer Al/Ti/Pd/Ag multilayer was then deposited onto the rear surface of the cell, and the cell was sintered. Finally, the top contact was electrolytically plated with silver, and a double-layer antireflection coating was deposited (ZnS/MgF_2). Three cells were fabricated on each two-inch (50.8-mm) diameter silicon wafer, from which they were cut using a laser scriber.

Since the cells were designed to be encapsulated under the prismatic covers, the MgF_2 antireflection layer serves no useful optical function in the final encapsulated cell. The ZnS/MgF_2 combination, however, produces a more rugged coating than ZnS by itself.

2.5 Initial Results

The final specifications for the cells for this project were sent from Sandia on 3 November 1987 and received by the project manager at the University of New South Wales (M.A. Green) on 16 November 1987. Masks were immediately designed and the completed tapes sent out for mask fabrication. The completed mask sets were returned on 23 December 1987, the last working day before Christmas.

A batch of cells was quickly processed. Two cells from this batch were chemically plated and dispatched without antireflection coatings to Sandia on 8 January 1988, less than two months after receipt of the final cell specifications. Another 36 cells with electrolytically plated silver and double layer antireflection (DLAR) coatings were dispatched on 28 January 1988.

The cells from this second batch were measured at Sandia on 2-3 February and three cells were sent to Entech for the application of prismatic covers. The covered cells were measured at Sandia on 17-24 February. Two important results were demonstrated by these cells.

The first was that the gain in current of the three cells upon application of the covers was consistent with their respective grid coverage fraction. This fraction was 15-17%, 17-18% and 20-23% for cells W476-2, Z784-2 and W745-1 respectively. The current gains were 15.5%, 16.2% and 20.6% respectively. The efficiencies also showed a similar increase, except for cell Z784-2, which improved very substantially upon covering. This may have been due to an initial mis-measurement, due possibly to poor contact to the cell. The differences between the maximum possible boosts of $f/(1-f)$, where f is the shading fraction, and the boosts observed experimentally are due to optical inefficiencies in the cover. These arise from reflection from the top surface of the cover augmented by steering of light onto the metallization fingers, particularly for the higher values of f.

Table 2.2 shows the gain upon covering in the "one-sun" performance of cell W476-2. Under high concentration, a decrease in fill factor would be expected upon covering at any given concentration ratio, due to increased series resistance loss arising from the increased cell current. This effect is demonstrated for the same cell in Table 2.3 at about 190-suns' concentration.

The second important result was that cell W476-2, although only about the 10th most efficient cell supplied in the batch of 36 cells, demonstrated an energy conversion efficiency above the target of 24% for concentration levels up to 140 suns.

The specific series resistance of five other cells supplied in the second batch was extracted from the behavior of the cell fill factors as the concentration level varied from 150 to 300 suns. This resistance varied from 4.2 ± 0.1 m Ωcm^2 for cell W476-3 to 10.4 ± 0.1 mΩ cm^2 for W472-3. Many cells had a value lower than the design value of 8 mΩ cm^2 for these 0.2 Ω cm substrates.

Additional cells were dispatched on 9 March, 15 March, 21 March and 5 April, bringing the total of cells supplied during this initial phase to 129. Processing then stopped until questions relating to the solderability of the cells were resolved.

Table 2.2: Gain in performance after applying a prismatic cover to cell W476-2 at "one-sun" concentration (measurements by Sandia National Laboratories).

Covered	V_{oc} (mV)	J_{sc} ($mAcm^{-2}$)	FF (%)	Effic. (%)
No	658	32.9	76.3	16.5
Yes	664	38.0	77.1	19.5
Gain	6mV	15.5%	1%	18%

Table 2.3: Gain in performance after applying a prismatic cover to cell W476-2 at 190-suns' concentration (measurements by Sandia National Laboratories).

Covered	V_{oc} (mV)	J_{sc} (Acm^{-2})	FF (%)	Effic. (%)
No	787	6.25	80.2	20.8
Yes	791	7.22	78.7	23.6
Gain	4mV	15.5%	-1.9%	13.5%

SECTION 3

3. SOLDERABILITY INVESTIGATION

3.1 Introduction

Despite the extremely encouraging efficiencies demonstrated by the initial cells supplied during the project, problems were experienced in solderability testing at Sandia. Two problems were reported during testing at Sandia during February and March:

(i) Low pull strengths of the top metallization when subjected to a pull strength test established at Sandia [3];

(ii) Marginal wetability by solder of both top and rear silver metallization of the cells.

The rear metallization strength was adequate, with failure under pull testing occurring at the titanium/palladium (Ti/Pd) interface. It was not clear whether the previous problems arose from intrinsic deficiencies in the cell metallization or from non-optimal soldering conditions for the particular metallization involved. With assistance from Clement Chiang of Sandia, Sandia soldering and pull-testing conditions as documented in Appendix A were duplicated at the University of New South Wales. The objective was to allow more rapid testing of metallization and experimentation with modifications to soldering conditions. A meeting was convened at University of New South Wales on 14 April involving all known staff with relevant experience to suggest possible approaches to overcome the reported difficulties. These were resolved by 24 May when two cells were dispatched to Sandia soldered directly to the copper plates that serve as heat spreaders in the Sandia Baseline Module design. To the top of the cell were soldered several of the copper tabs used in pull testing. These all passed the Sandia pull test exceeding 10 pounds of pull force (corresponding to an average force per unit area of 1,600 p.s.i. or 1.1×10^7 Nm^{-2}).

3.2 Rear Contact Metallization

Four processing changes were made that greatly improved both the wetability and adherence of the rear metallization.

The failure of the rear metallization at the Ti/Pd interface was attributed to the fact that vacuum was broken between Ti and Pd evaporations. This was for processing convenience since only two metals could be evaporated each vacuum pumpdown. Hence, Al/Ti was evaporated in the first cycle, followed by Pd/Ag in the second. The first change implemented was to deposit the rear metal in three vacuum pumpdowns so that Al was deposited first, followed by Ti/Pd, and finally Ag.

Since dissolution of the Ag in the 62.5% Sn 36.1% Pb 1.4% Ag solder used was thought to be one reason for the poor wetability of the rear, the second change was to increase the thickness of Ag evaporated on the rear from 0.5 microns to above 4 microns.

The third change was in sintering ambient from N_2 to forming gas (N_2/H_2). This reduces the tendency of the Ag to oxidize during this step.

The fourth change was to shade the rear of the cells during the antireflection coating step. This was to eliminate deposition of dielectric material on the rear during this step.

3.3 Top Contact Metallization

The change in sintering ambient noted above had similar benefits for the top contact. Since aluminum was not evaporated for the top contact metallization scheme, no vacuum break occurred between titanium and palladium evaporations so no changes were required in this area.

The top contact adhesion problem seemed the most difficult but was solved in a surprisingly simple way. Normally, the copper tab soldered for pull-testing is soldered right up to the edge of the busbar, as in Figure 3.1. Upon pulling the contact, the highest stress is concentrated at the edge of the busbar. If the metal lifts in these areas, stress is concentrated at the edge of the region remaining intact. Hence, once the metal lifts, the contact will fail by a peeling action at a relatively low applied force.

One way to minimize the peeling problem is to prevent the metal

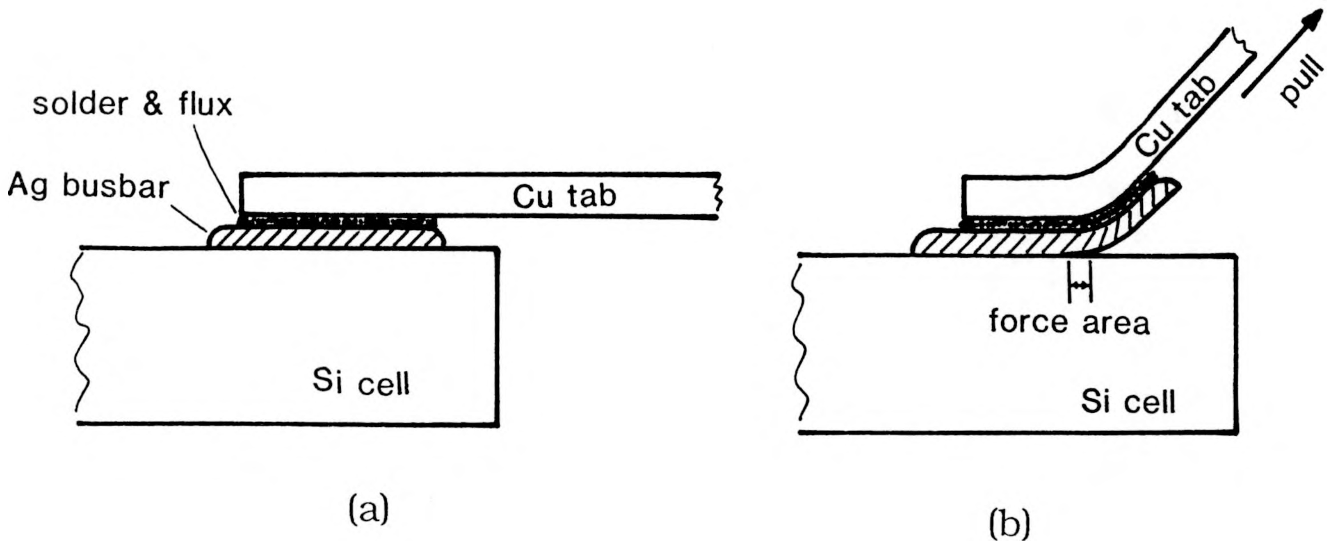

Figure 3.1: Normal soldering approach for cell interconnects

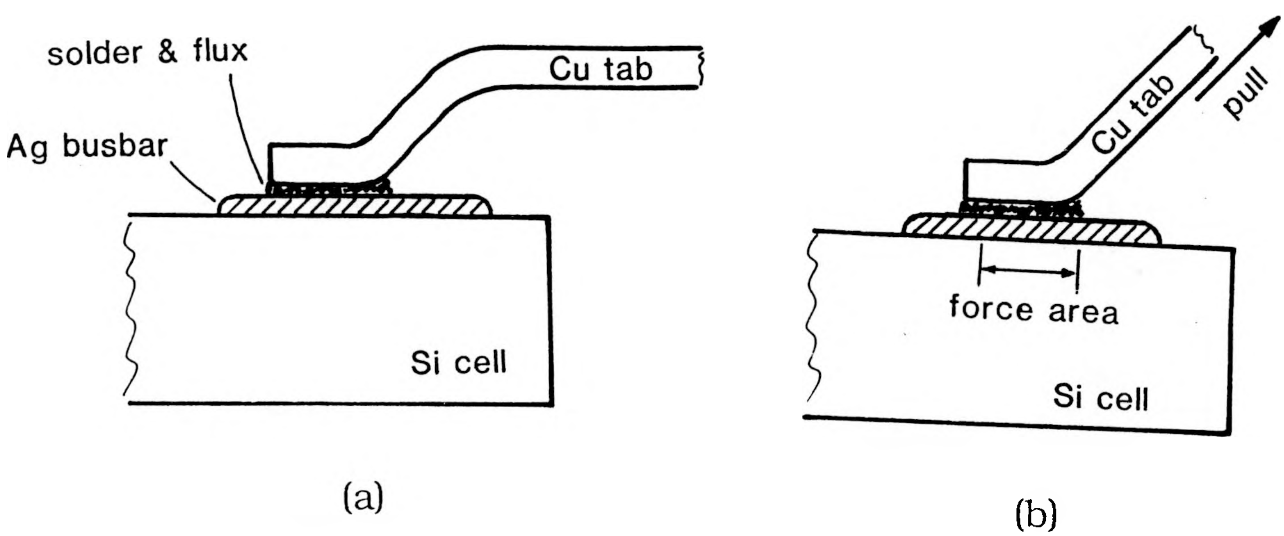

Figure 3.2: Recommended soldering approach

from lifting. The edge of the busbar is not a good place to concentrate pull stresses since it is likely to be the place of weakest adhesion between the metal layers and the cell. This is due to effects at the edges, such as interfacial regions of the layers being the most heavily oxidized in these areas and the potential for attack of these interfacial regions by fluxes used in soldering.

By the simple expedient of soldering the contact only to regions well away from the edge of the busbar as in Figure 3.2, contact pull-strength can be greatly improved. Not only are the forces tending to make the metal lift spread over larger areas, they act at areas of better adhesion than at the edges. Experimentally, the pull strength increased by a factor of more than 20 by this approach. Contacts formed in this way do not fail at the maximum force at which they were tested of 10 pounds (1,600 p.s.i. or 1.1×10^7 Nm^{-2}) compared to the value of about 4 pounds (640 p.s.i. or 4×10^6 Nm^{-2}) believed acceptable for mounted cells to pass qualifications testing.

Two approaches have been demonstrated for preventing the busbar being contacted right up to its edge. One is to use preformed tabs bent so as not to contact the busbar near the edges. A second is to prevent the solder from wetting the busbar in these regions by having them covered by a suitable non-wetting layer. Arranging for the cell antireflection coating to overlap the busbar in these regions may be a way of implementing the latter approach.

3.4 Summary

Although problems were experienced with soldering to the initial cells delivered in the project, relatively minor processing changes eliminated these difficulties.

The most striking change was the demonstration of the enormous gain in strength if interconnections soldered to the top busbars were not soldered right up to the edge of these busbars.

Cells fabricated after mid-May incorporated the changes outlined above and divided the cells supplied during the project into two groups: the 129 cells supplied before this date and the 422 cells supplied after this date, described in the following section.

SECTION 4

4. CELL PERFORMANCE CHARACTERISTICS

4.1 Introduction

In addition to four cells dispatched to Sandia on 24 May in connection with the soldering studies of the previous section, a further 418 cells were dispatched in five large batches between June and October 1988. These batches were designated "UNSW 1" to "UNSW 5". A summary of the available performance characteristics of these cells compiled at Sandia is given in Appendix B and Appendix C.

All cells were measured at "one-sun" and 190 suns' concentration prior to application of the covers, while some were also measured at 125 suns or across a wide range of concentrations. Data on approximately 40 of these cells, after application of the prismatic covers, were also available at the time of report preparation.

Of the uncovered cells, about 270 of the 418 demonstrated an efficiency above 20% at 190 suns, with 116 of these being above 21%. The highest efficiency seen at this concentration ratio was 22%. Soldering to the copper plate caused no change in 36 of the 40 cells to within the measurement repeatability of about 2% (relative). Of the remaining four cases, efficiency went down by more than this margin in three cases and up in the remaining one. Of the 37 cells for which all necessary data were available, application of the prismatic covers increased the ratio of efficiency at 190-suns concentration before and after covering by 13.1%. The ratio of efficiency at 125 suns after covering to that at 190 suns before covering increased by 14.9%, nearly the same value as the average measured metallization fraction for these cells of 14.8% ± 1% .

Twelve of the 40 covered cells demonstrated 24% efficiency in the concentration range of interest (125-190 suns), with 25% being the peak demonstrated. The highest efficiency cell to which a cover had been applied at the time of report preparation had an efficiency of 21.8% at 190 suns prior to soldering compared to the value of 22.1%, which was the highest of all cells supplied at this concentration. The lowest efficiency cell to date to demonstrate 24% efficiency after cover application had an efficiency of 20.4% at 190 suns prior to cover application.

4.2 One-Sun Versus Multi-Sun Performance

Initial screening of the cells at University of New South Wales was at "one-sun" illumination levels. Cells were dispatched to Sandia graded on the basis of "one-sun" performance. This made it particularly apparent that there was often not a strong correlation between one-sun efficiency and efficiency under concentration. On several occasions a cell with poor one-sun performance performed astoundingly well under concentration.

One reason for this is shown in Figure 4.1, which shows the output characteristics of one such cell at "one-sun" and at 190-suns' concentration. Although the output curve under concentration is nearly ideal, that at "one sun" is far from being so. It can be interpreted in terms of the equivalent circuit of Figure 4.2.

The main cell is represented by the large diode. In parallel is a Schottky diode in series with a reasonably large resistance. The source of this branch of the circuit is believed to be pinholes in the oxide pad upon which the busbar sits. These pinholes most likely would arise from defects to which the photolithographic masks are prone after extended use. Metal contact would extend through the pinhole to the undoped silicon surface giving rise to the Schottky diode. The series resistance could arise from the spreading resistance of this diode given by $\rho/2d$ where ρ is the substrate resistivity and d the pinhole diameter.

At low forward bias both diodes block current flow. As the "knee voltage" of the Schottky diode is approached, it begins conducting current. This gives rise to the hump at about 0.3V in the "one sun" characteristics. As the voltage increases further, the main cell diode begins conducting in the normal way.

At high concentration levels, the series resistance of the Schottky diode restricts currents through it to negligible levels. The characteristics then revert to the nearly ideal form apparent at 190 suns in Figure 4.1.

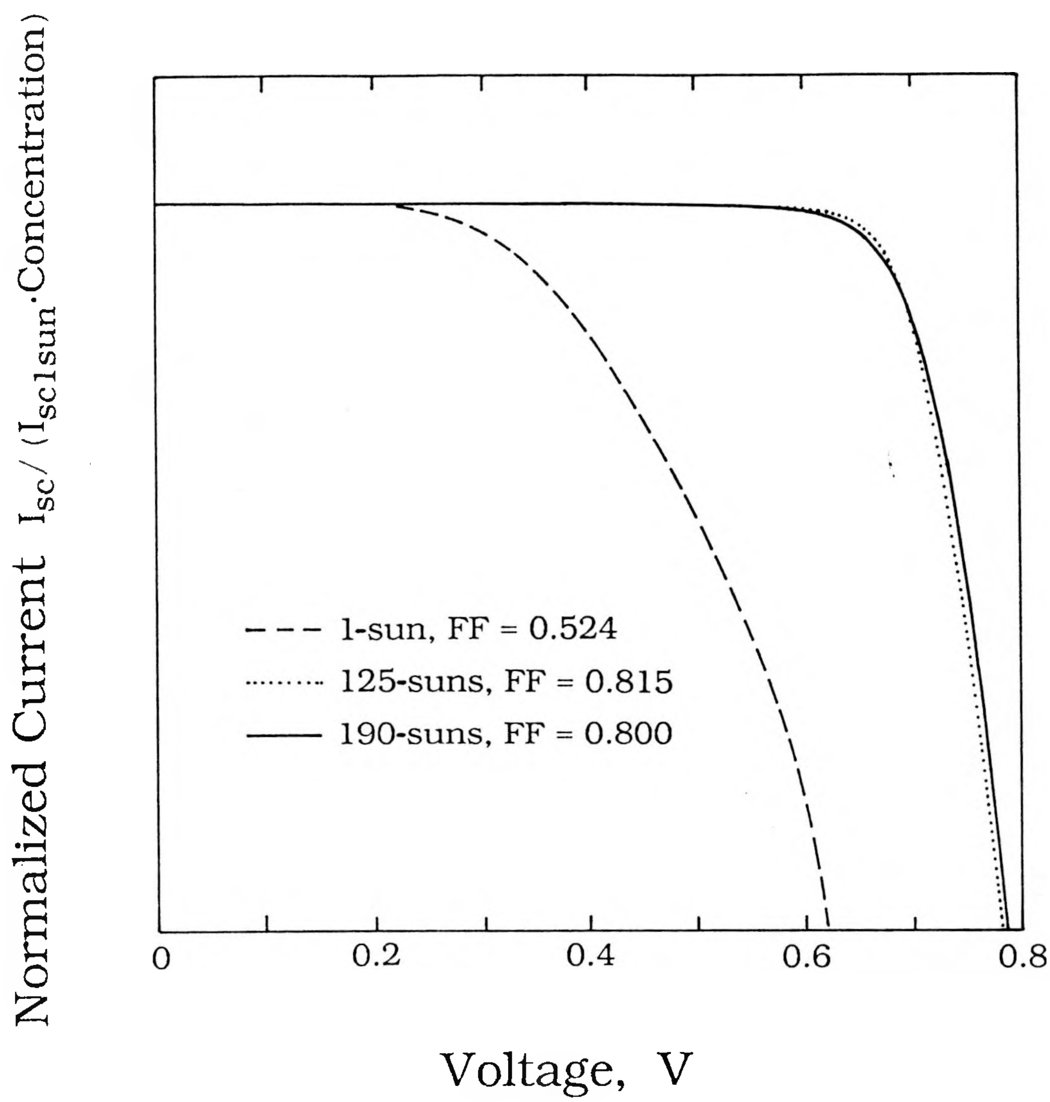

Figure 4.1: Output characteristic of a partially shunted cell at one-sun, at 125-suns' concentration and at 190-suns' concentration.

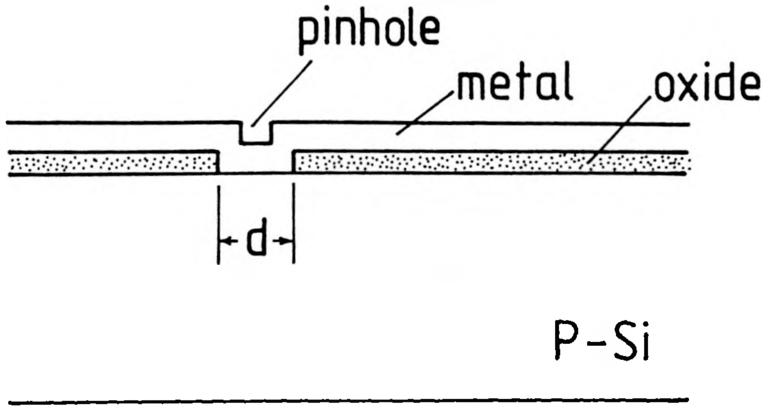

(a)

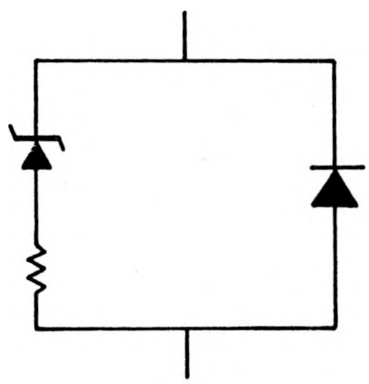

(b)

Figure 4.2: Equivalent circuit of partially shunted cell

4.3 Uncovered Results

The distribution of measured efficiencies at both one-sun and 190-suns' concentration is shown in Figure 4.3. Maximum efficiencies observed were 19% and 22% respectively, with median values of 17.6% and 20.5%. Since the contract called for the supply of "mechanical" samples and electrically active cells, virtually all cells processed to completion are included in this sample.

4.4 Covered Results

A sketch of a cell after application of the prismatic cover is shown in Figure 4.4. The curvature in the regions above the fingers steers light away from these fingers, correspondingly increasing cell output current.

At the time of report preparation, data were available for the effect of application of prismatic covers for about 40 cells. These were all from batches UNSW 1, 2 and 3. The results of testing after such covers were applied are summarized in Appendix C. As noted previously, the covers demonstrated very high optical efficiency when tested under the reasonably well-collimated light from the solar simulator.

The average metal coverage of the cells for which full data were available was 14.8% ± 1% as measured at Sandia, very close to the design value of 15%. The average boost in efficiency of soldered cells at 190-suns' concentration after application of the covers was 13.1%. Some of the difference between these figures can be attributed to increased resistance loss due to the higher cell currents after cover application. From the additional fact that the boost in performance at 125 suns after covering over that at 190 suns before covering was 14.9%, it was deduced that about 0.8% of the difference previously noted was due to this effect.

This high optical efficiency is quite surprising when the optical mismatch at the cover/air interface is taken into account. This would be expected to be similar to or slightly larger than that at the unmetallized region of the uncovered cell. There would be additional reflection from the adhesive/cell interface after covering. Therefore, even if the covers did a perfect job of steering light away

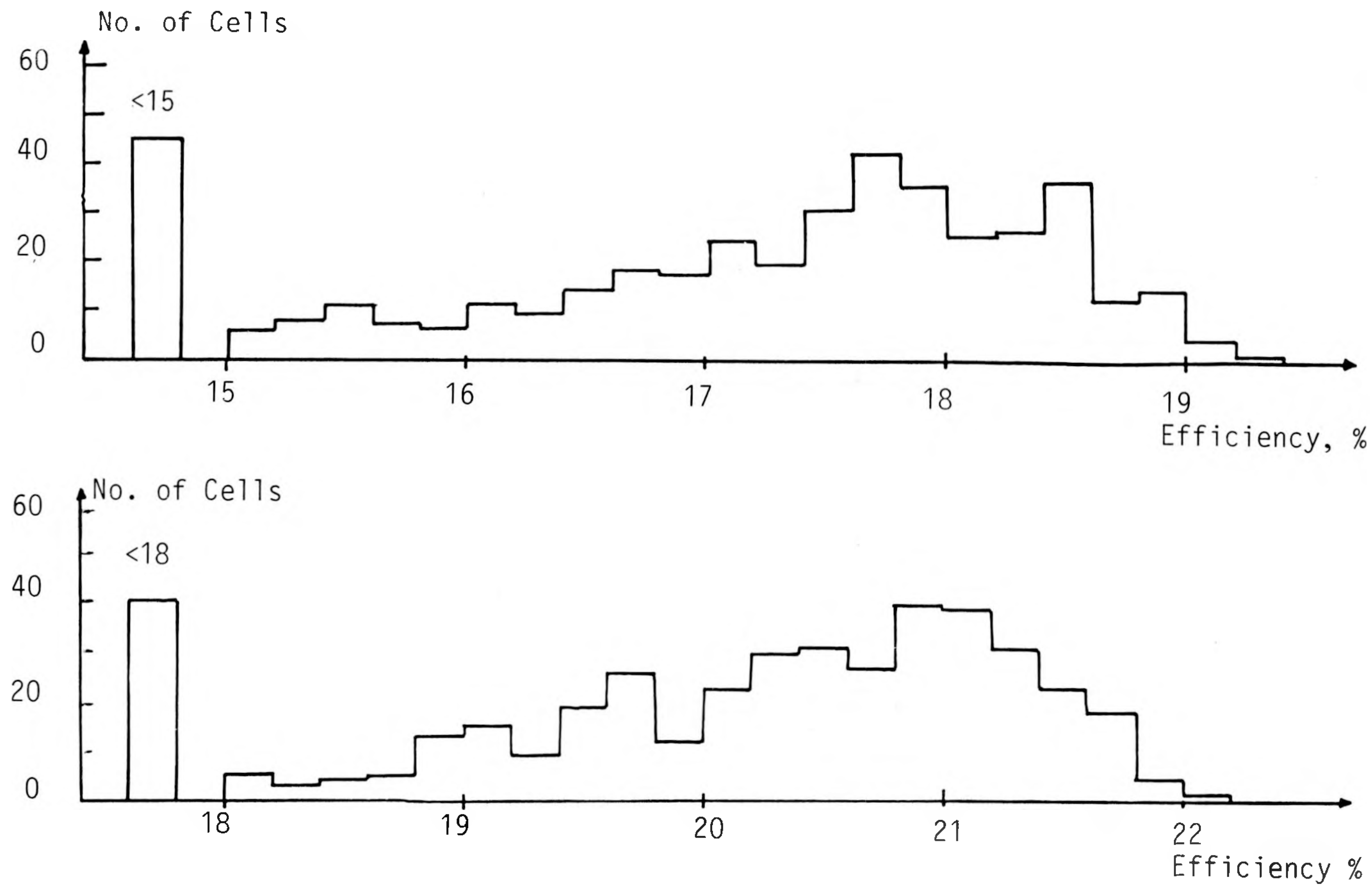

Figure 4.3: Distribution of measured energy conversion efficiencies of cells prior to application of prismatic covers: (a) at one sun; (b) at 190-suns' concentration.

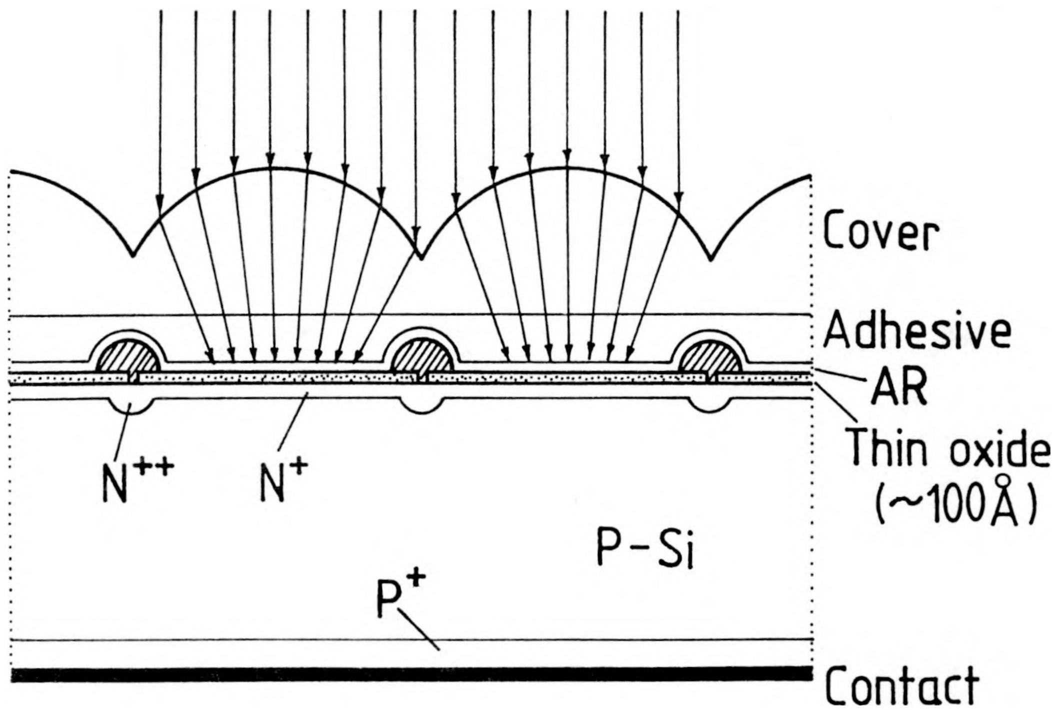

Figure 4.4: Sketch of cell after application of a prismatic cover

from the top metallization, the gain would be expected to be smaller than the metallization coverage fraction due to increased reflection loss.

The fact that the observed gain is so high suggests that another mechanism may be at work reducing reflection loss. The cover may form, in combination with the microgrooved cell surface, a light trapping structure similar to the "perpendicular slat" structure analyzed elsewhere [4]. At least some of the light reflected at the cell/adhesive interface may be trapped by this structure to have a second chance of being coupled into the cell. If this proves to be the case, it may be possible to use cells with simpler silicon dioxide antireflection coatings. This would simplify cell processing as well as eliminating a small amount of UV absorption, that occurs in the ZnS layer of the present cells.

The highest efficiency cell measured to date after application of prismatic covers was cell W471-2. This was the 16th most efficient cell supplied during the project, based on Sandia measurements at 190 suns. There are prospects that higher efficiency will be posted when all cells have been covered.

Cell W471-2 had a measured metallization coverage of 14.8%, close to both the design point and the average of cells measured to date. Prior to application of the prismatic cover, the cell displayed an efficiency of 21.6% at 190 suns both before and after soldering. After application of the cover, this efficiency increased by 15.1% (relative) to 24.8% at 190 suns. This figure was subsequently revised to 25.0% when corrected for spectral mismatch between the simulator and the reference direct beam AM1.5 spectrum (ASTM E-891).

The measured hemispherical reflection from the cell with prismatic cover applied when illuminated perpendicularly by light of different wavelengths is shown in Figure 4.5. This includes reflection from all sources including the top surface of the prismatic cover, the cover adhesive/cell interface, and from the metallization fingers, if light were being steered onto these. The low value of this reflection right across the spectrum is one reason for the high current densities shown by these cells.

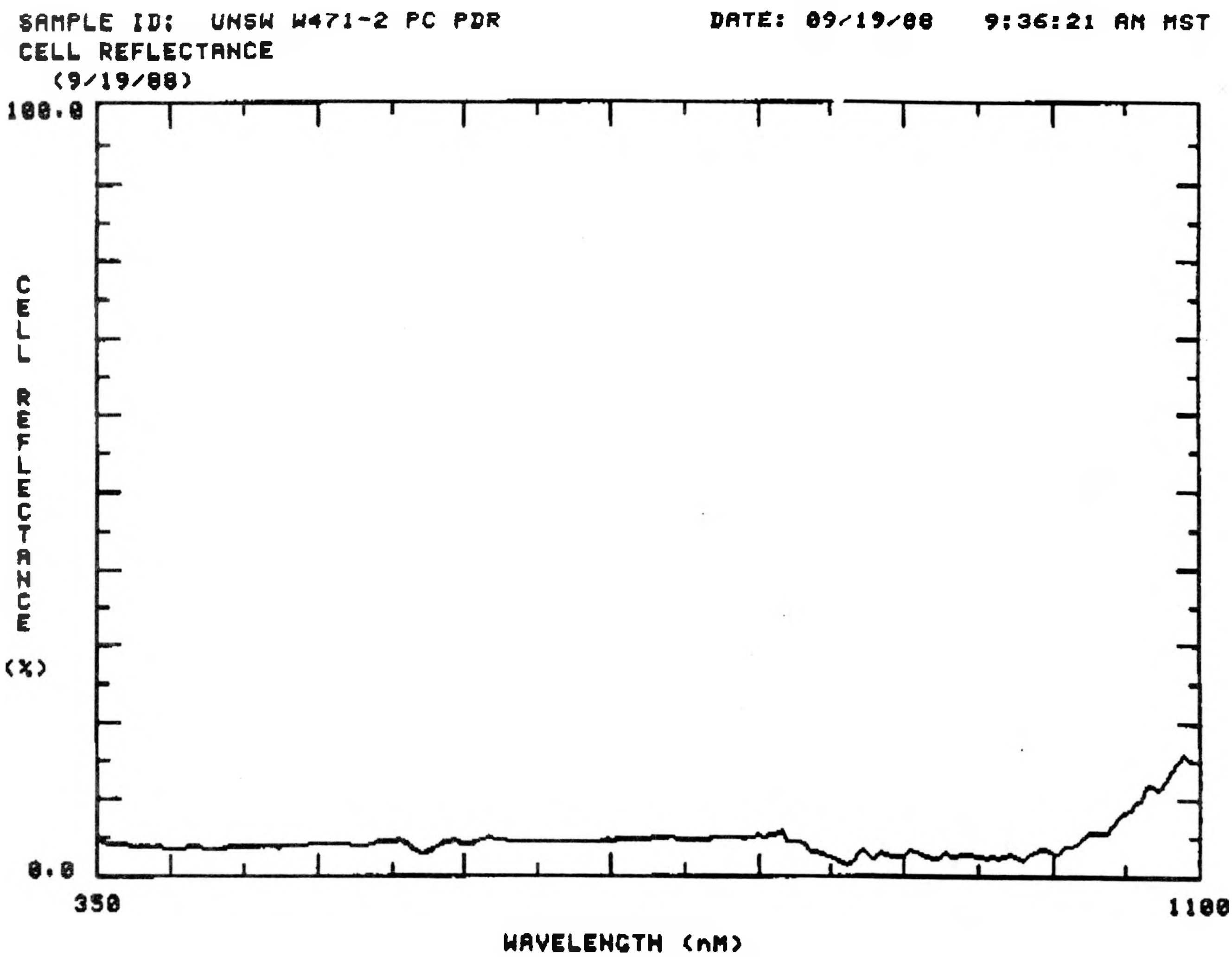

Figure 4.5: Hemispherical reflection versus wavelength for cell W471-2. Measurements by Sandia National Laboratories.

The measured external responsivity and corresponding internal quantum efficiency as a function of wavelength are shown in Figure 4.6(a) and (b). The external responsivity is combined with the measured spectral irradiance of the solar simulator to calculate the spectral mismatch factor for the cell, a factor by which the apparent efficiency has to be multiplied. This factor was calculated at Sandia to have the value 1.0112. The internal quantum efficiency shows a good response for this cell right across the spectrum. Since the internal response is similar to that of the cell prior to application of the covers, it is deduced that there is not strong absorption of light in the cover. The falloff apparent at short wavelengths is due to absorption in the ZnS antireflection coating layer.

Table 4.1 shows the measured performance of this cell as a function of concentration ratio. The cell maintains an efficiency above 24% across the whole range of concentration ratios from 20 to 250 suns. The efficiency is above 25% between 100 and 200 suns.

4.5 Outdoor Testing

Outdoor testing at Sandia of covered cells revealed that the acceptance angle of the covers was not as large as the design value for one direction of the incident light. This was attributed to the cover plus adhesive thickness being larger than the design value.

Despite this limitation the cells performed creditably under outdoor testing. Combined with a 12.5-cm square Fresnel lens of the type described elsewhere [5], a combined lens/cell efficiency of 20.4% was demonstrated. The output of the cell (Cell W55C-3) under such testing is shown in Figure 4.7 (100.0 mW/cm^2 direct normal insulation on lens, 20°C cell temperature). The measured lens/cell efficiency of 20.4% was in this case partitioned between lens and cell as 86.5% lens efficiency and 23.5% cell efficiency. The latter is slightly lower than the measured efficiency when tested under the simulator indoors of 23.7% at 190-suns' concentration. The non-uniform illumination in the lens/cell testing would tend to reduce cell efficiency. Another contributor to reduced efficiency could be the less than ideal operation of the prismatic cover under non-collimated light, due to the thickness reportedly being off specification. Although it does not represent a

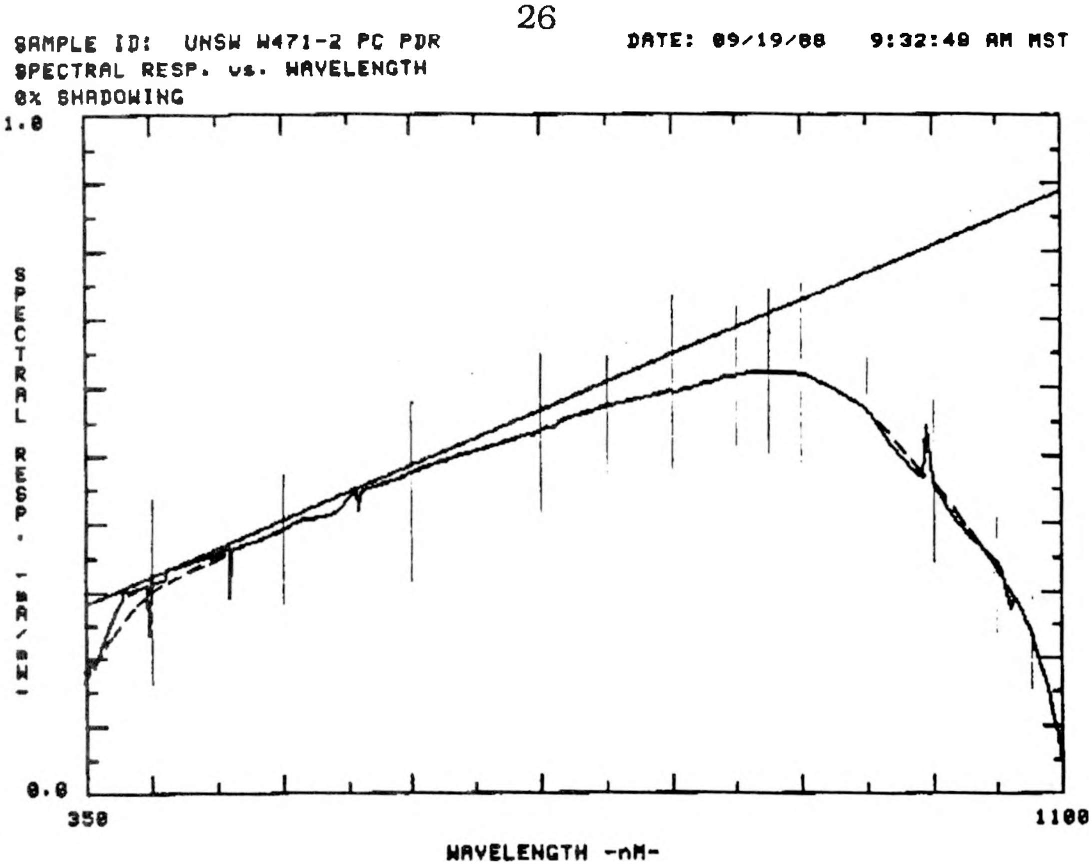

(a)

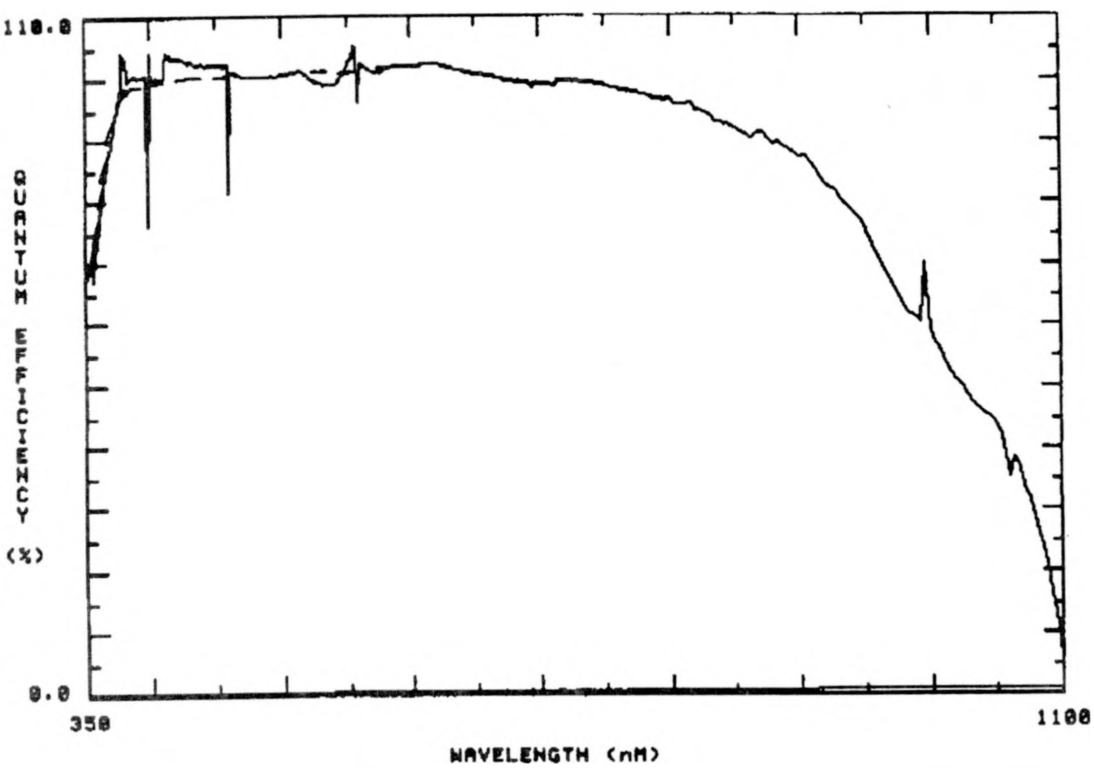

(b)

Figure 4.6(a): Measured external responsivity, (b): corresponding internal quantum efficiency. Measurements by Sandia National Laboratories.

Table 4.1: Measured performance of cell W471-2 as a function of concentration level after application of prismatic covers. Measured at Sandia National Laboratories under the direct beam AM1.5 spectrum (ASTM E-891 at 25°C). Responsivity of the cell is 0.0392 A/W.

SUNS	V_{OC} (mV)	FF (%)	EFFIC. (%)
1	666	81.3	21.2
20	743	83.8	24.4
102	780	82.3	25.2
203	792	79.8	24.8
248	796	78.1	24.4

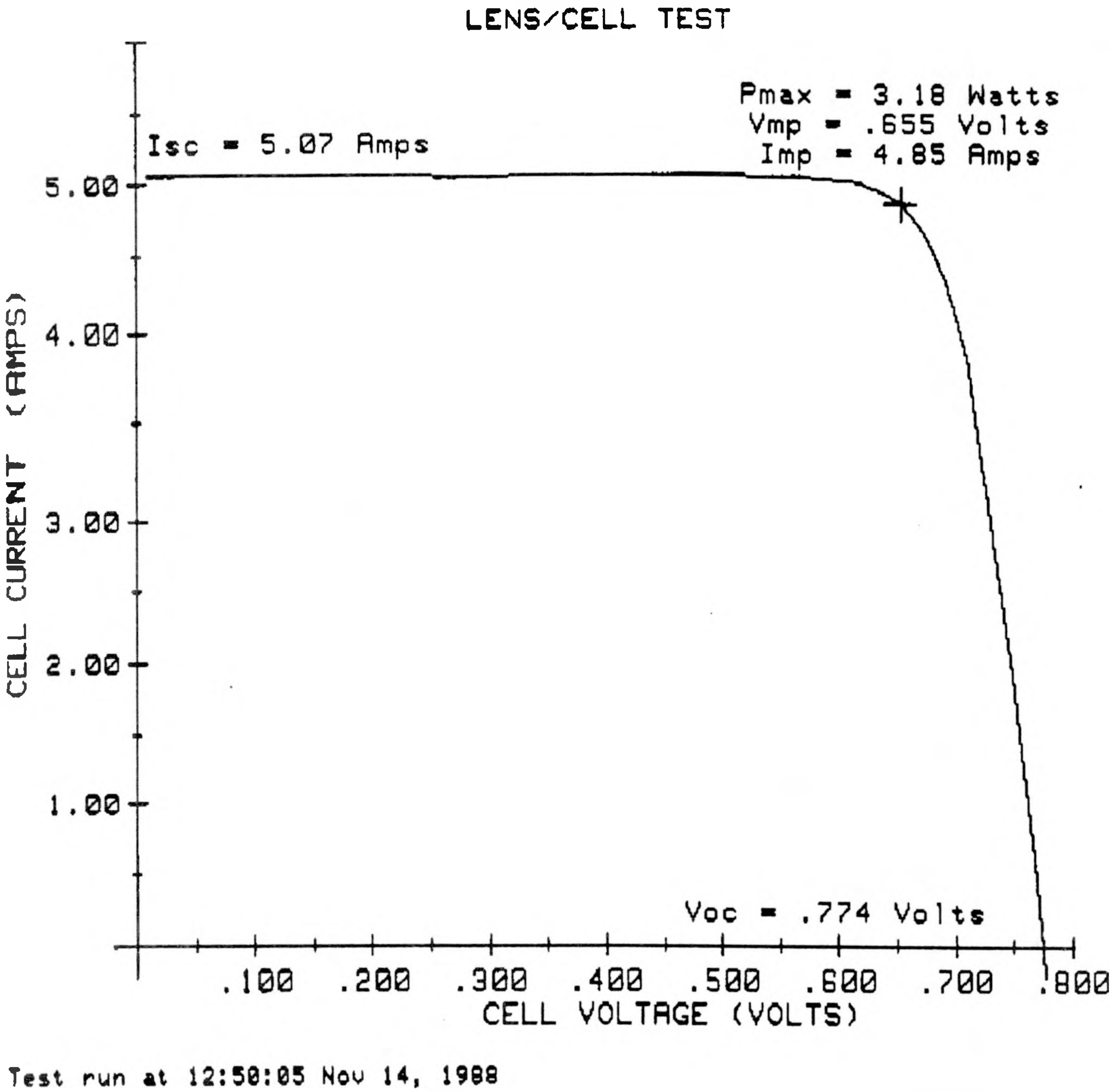

Figure 4.7: Output characteristics of Cell W55C-3 measured in outdoor lens/cell testing at Sandia National Laboratories.

limit on what is possible with the cells supplied under the present project, the 20.4% lens/cell efficiency demonstrated is believed to represent a significant improvement over the previously highest value of lens/silicon cell efficiency measured at Sandia. This is believed to be the value of 19.0% established using cells supplied under an earlier University of New South Wales project (Sandia Contract 01-8551), which itself was a substantial increase over earlier results.

ENTECH also conducted experiments with another cell using several different lenses. Best results were obtained with a linear Fresnel lens designed for 22X concentration. The cell would undoubtedly give its highest efficiency at higher concentration levels than this. However, lens efficiency may be higher at the lower concentration levels.

The prism cover may also work more effectively at the lower concentration levels if the cover plus adhesive were thicker than specified, since a smaller range of incident angles would be expected at the lower levels. A combined lens/cell efficiency over 20% was measured at 22X concentration [6].

Twelve of the cells supplied during this project were subsequently incorporated into a module developed at Sandia National Laboratories [5] to set a record efficiency for a photovoltaic concentrator module. The cells were covered with prismatic covers designed by ENTECH and molded directly to the cells at Sandia. The performance of the cells and the module is briefly summarized in Table 4.2, as supplied by Sandia.

The module efficiency adjusted to a cell temperature of 25°C is plotted as a function of direct normal irradiance in Figure 4.8 as measured at Sandia National Laboratories. This experiment demonstrated both the high efficiency and the suitability of the cells for use in a module.

4.6 Future Improvements

Further improvements in silicon "module ready" cell performance are likely as cell structures evolve. The next generation of University of New South Wales cell, the PERC cell (passivated

Table 4.2: Cell and Module Performance - Sandia 20% Experimental Module

Optical Efficiency	:	86.5 to 87.5%
Cell Indoor Efficiency	:	24.4% (85 suns, 25°C)
Current	:	38.1 mA/cm^2 (1 sun)
Open-Circuit Voltage	:	.772 V (85 suns, 25°C)
Fill Factor	:	.829 (85 suns, 25°C)
Cell Outdoor Efficiency	:	23.0% (85 suns, 25°C)
Module Outdoor Efficiency	:	20.3% (80 mW/cm^2, 25°C)

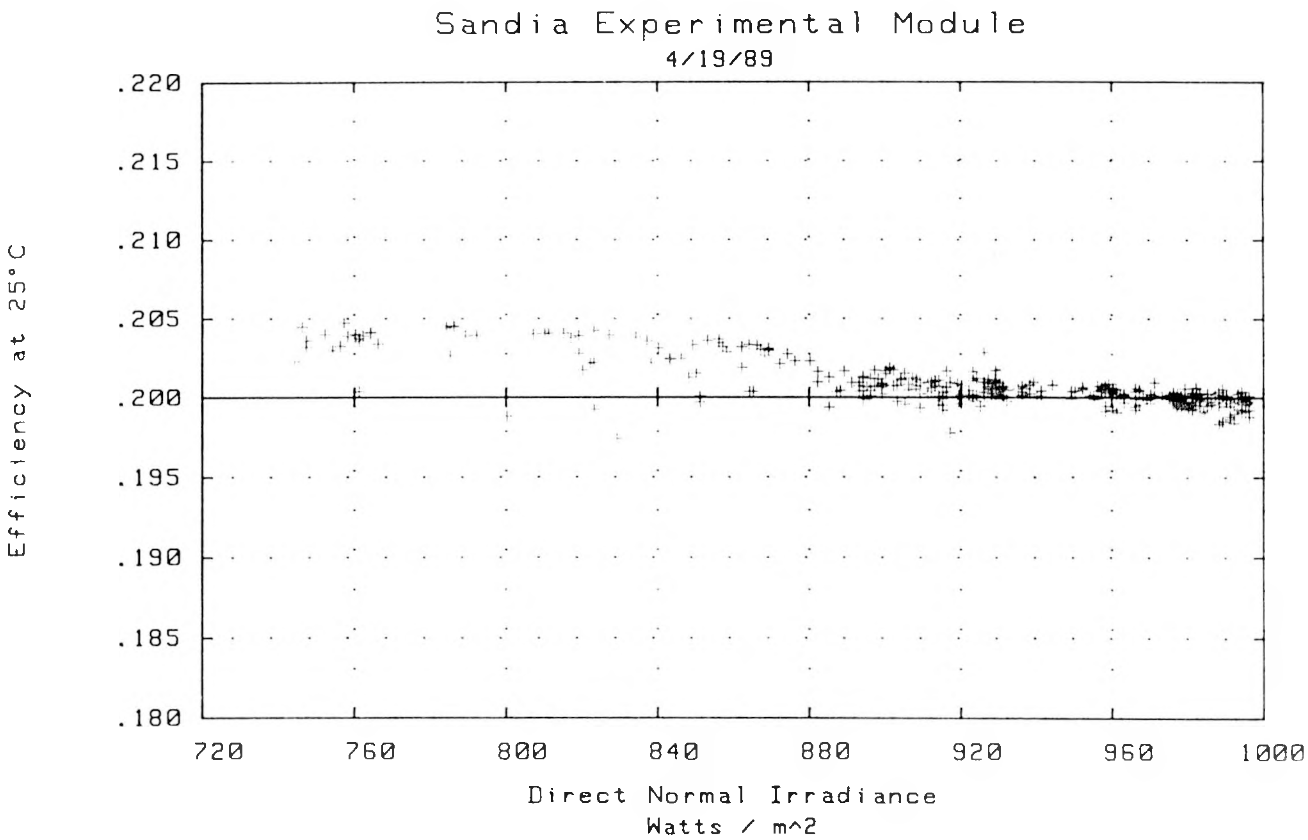

Figure 4.8: Efficiency at 25°C cell temperature versus direct normal irradiance for Sandia 20% Experimental Module incorporating twelve cells supplied duirng the present project.

emitter and rear cell) has recently been demonstrated. Although not yet optimized for concentrator cell applications, the first cells have now been fabricated using the mask set generated for the present project. These demonstrated higher efficiency at "one sun" than the cells supplied during the present project. However, these particular cells did not perform well under concentration due to non-optimized resistive components [7].

The cells supplied during the present project had only 15% metal coverage. By minimizing the range of angles the cells have to accept by using, for example, longer focal length lenses, it may be possible to increase this coverage with consequent benefits to cell performance.

The present prismatic covers apparently do not incorporate an antireflection coating for the cover/air interface. This could be a worthwhile addition if a suitable coating method could be found.

The cells supplied during the present project would also be suitable for other schemes that reduce the effect of top metallization coverage. For example, the scheme such as suggested by Stanford University [8] would fall into this category. Light is focused through a small opening into a reflective box placed over the cell. By concentrating light a factor of M higher than the geometric concentration ratio (lens/cell area ratio) to focus it through the opening, net refection would ideally be reduced by this factor and the effectiveness of light trapping schemes correspondingly increased.

SECTION 5

5. Conclusion

This project demonstrated the feasibility of producing 24% "module ready" silicon concentrator cells in reasonably large quantities. A peak efficiency of 25.2% was demonstrated during the present project within the designed concentration range.

Prismatic covers were shown to possess almost anomolously high optical efficiency when tested under the reasonably well collimated light from a solar simulator. Testing at Sandia indicated that this efficiency may be somewhat lower for light of a wider range of incident angles. It is possible to design the covers to perform ideally under a range of different incident angles. The present disparity is attributed to a combined cover/adhesive thickness larger than specified.

Even with this limitation, outdoor testing gave combined lens/cell efficiency over 20%, believed to be the highest value ever reported using silicon cells. This result confirms the feasibility of fabricating 20% efficient silicon concentrator modules. Subsequently, twelve cells supplied during the project were incorporated into an experimental module developed by Sandia which demonstrated 20.3% efficiency (80 mW/cm^2, 25°C cell temperature). This appears to be the first photovoltaic module to surpass the 20% efficiency milestone.

Much higher module efficiencies are possible with improved efficiencies of the optical elements and improved cells. In the latter area, a new generation of cell with improved electronic and optical performance, the PERC cell, has recently been demonstrated at University of New South Wales. Cells of this type and the present size are believed capable of demonstrating cell efficiency in the 26-27% range under concentration at their present stage of development.

SECTION 6

6. References

1. P.A. Basore, Sandia National Laboratories, private communication.

2. M.A. Green, J. Zhao, A. Wang, A.W. Blakers, C.M. Chong, F. Zhang, A. Sproul, S.R. Wenham and P. Campbell, "*Silicon Concentrator Solar Cell Research,*" Report SAND88-7032, Sandia National Laboratories, Albuquerque, December 1988.

3. C.J. Chiang and E.H. Richards, "*Reliability Research and Cell Assembly Design for Photovoltaic Concentrator Modules,*" Conf. Record, 19th IEEE Photovoltaic Specialists Conf., New Orleans, May 1987, pp. 1222-1227.

4. P. Campbell and M.A. Green, "*Light Trapping Properties of Pyramidally Textured Surfaces,*" J. Appl. Physics, Vol. 62, pp. 243-249, 1987.

5. D.E. Arvizu, "*Development of the Sandia 200X Experimental Silicon Module,*" Conf. Record, 17th IEEE Photovoltaic Specialists Conf., May 1987, pp. 805-813.

6. M.J. O'Neill and A.J. McDanal, "*Outdoor Testing of a 21% Efficient Single-Cell Laboratory Concentrator Module, Comprising a Linear Fresnel Lens, Prism Cover, and Microgrooved Silicon Cell,*" Conf. Digest, 4th International Photovoltaic Science and Engineering Conference, Sydney, February 1989.

7. M.A. Green, A.W. Blakers, J. Zhao, A. Wang, A.M. Milne, X. Dai and C.M. Chong, "*High Efficiency Silicon Concentrator Solar Cell Research,*" Report SAND89-7041, Sandia National Laboratories, Albuquerque, December 1989.

8. R.A. Sinton and R.M. Swanson, "*Increased Photogeneration in Thin Silicon Concentrator Solar Cells,*" IEEE Electron Device Letters, Vol. EDL-8, pp. 547-549, 1987.

APPENDIX A

SANDIA SOLDERING TECHNIQUE

(Letter from Clement Chiang to M.A. Green)

Sandia National Laboratories
Albuquerque, New Mexico 87185

April 15, 1988

Professor Martin Green
University of New South Wales
Anzac Parade Street
Kensington, NSW 2033
AUSTRALIA

Dear Martin:

This letter describes the materials, tools, and procedures that I use for testing the adhesion of solar cell metallization to the body of solar cells. The details of this procedure are presented in the following order:

1. Materials
2. Tools
3. Procedure
4. Some results

I am sending you, by express shipping, the materials and tools listed below that are marked with an asterisk.

Materials

1. *Copper tabs: OFHC (oxygen free high conductivity) copper .010" thick, .394" long, .079" wide cleaned with an acid etch (15% HNO_3 together with 15% H_2SO_4, DI water rinse followed by propanol rinse, blow dry)

2. Solar cells: your choice

3. Copper substrates: .0625" or thicker is fine
If dirty, clean with the acid etch.

4. *Solder sheet: alloy Sn62 (62.5% Sn, 36.1% Pb, 1.4% Ag) .001" thick

5. *Rosin flux: no activation is needed for wetting clean copper and clean silver. Activators often can attack the antireflective coating of cells.

Tools

1. *Hemostat: locking forceps with serrated jaws
2. *Spring scale: to ten pounds force
3. Hotplate: with temperature control to ±10 degrees C
4. *Transfer pipet: one piece polypropylene
5. *Razor blades
6. *Glass slides
7. *Diamond pencil and glass cutter
8. *Teflon sheet
9. Forceps
10. Propanol
11. Pliers
12. Vise

Procedure

In general, do not handle the parts to be soldered; doing so leaves a film of undesirable stuff. Always be on the lookout for dirt particles.

1. Cut the sheet solder using the razor blade, with the solder placed on a glass slide. Use a glass slide as a guide.

    a. strips of solder for the cell busbars
    b. a square of solder for between the cell and the substrate

2. Using a transfer pipet, place a small dot of flux on the cleaned substrate and squish this to a thin film using a piece of teflon sheet.

3. Place the square piece of solder on this film of flux.

4. Use the teflon to press the solder to the substrate, thus coating the bottom of the solder with flux. Flip the piece of solder over and repeat.

5. Place the cell on the flux-coated piece of solder.

6. Repeat steps 2 through 4 using the solder strips, with the desired end result being strips of flux-coated solder on the cell busbars.

7. Place the ends of the copper tabs on the strips of solder and hold the tabs in place with a piece of a glass slide, cut to size by breaking along a line scribed by the diamond pencil. It may be helpful to place a small weight on the glass.

8. Place the substrate on the hotplate, which has been conveniently preheated to a temperature of 210 degrees C.

9. Use the forceps to prevent the tabs from moving around when the solder melts, as they so often like to do.

10. Smoothly, glide the substrate over to the edge of the hotplate and remove it using the pliers.

11. Place the substrate on a chunk of metal until it cools.

12. Remove any small amounts of residual flux with the propanol.

13. Clamp the substrate in a vise.

14. Bend the tabs to an angle of 45 degrees.

15. Clamp the hemostat to the end of the tab.

16. Hook the spring scale to the center axis of the hemostat.

17. Pull until something breaks.

Some Results

I have tested metallized silicon chips made by Charlie Chu of ASEC. The force required to pull off the metallization ranged from 2 to 10+ pounds, with an average value somewhere around 6 pounds. Often, the metallization remained intact at 10 pounds force, the limit of my spring scale.

However, a second batch of metallized chips made by ASEC didn't do as well, with an average pull strength of about 3 pounds. Charlie has informed me that metallization adhesion for these silicon chips represents the limit for real solar cells.

Mike Nowlan at Spire commonly measures a pull strength of 300 to 400 grams. However, he pulls at an angle of 90 degrees (this is much worse than 45 degrees) and uses tabs with a width of .100 inches instead of .079 inches. Like ASEC, Spire uses evaporated contacts.

In general, I have observed extremely wide variation in metallization adhesion. This is a serious problem shared by all makers of cells, particularly concentrator cells. Since a practical and non-destructive test for adhesion is not available, the yield of cells with good adhesion must be improved.

I would guess that for our application, a pull strength of 2 to 3 pounds would be sufficient, when measured using the above procedure. I believe this range includes a considerable margin of safety. Actually, I would be very happy if you could achieve a uniform pull strength of 2 pounds. I am presently conducting an experiment to determine the effect of thermal cycling on metallization adhesion.

Good luck; let me know what happens,

Clement

Clement Chiang

Copy to:

6221 all
6224 D. L. King

PS. I have been having trouble removing the ink that you use to mark the backs of cells. Could you please use an ink that can be completely removed by propanol or methanol? Thanks

APPENDIX B

SANDIA MEASUREMENT SUMMARY FOR BARE CELLS

(BATCHES UNSW 1-5)

UNSW1
BARE-CELL DATA

CELL ID	BOX#	EFF @ 1 SUN	EFF @ 125X	EFF @ 190X	GRID LINE %
W571-2	1	18.12		20.44	
W571-3	1	17.72		20.45	
W573-1	3	16.35		19.77	
W573-2	3	15.90		20.14	
W573-3	2	16.86		19.95	
W574-1	1	17.08		19.06	
W574-2	6	15.86		18.85	~17?
W574-3	1	16.81		18.64	~17?
W575-1	6	13.85		18.85	17.2
W575-2	6	16.42		19.47	16.0
W575-3	2	17.29		19.14	
W591-1	2	17.93		20.93	
W591-2	3	15.60		20.36	
W591-3	3	16.05		20.17	
W593-1	5	17.15		19.25	
W593-2	6	15.25		19.29	
W593-3	6	14.07		19.00	
W594-1	4	13.55		20.45	14.0
W594-2	4	17.74		18.95	
W594-3	4	15.49		20.13	
W595-1	2	14.98		19.56	
W595-2	1	19.08		19.81	
W595-3	2	17.28		19.46	
W597-1	2	17.50		20.18	
W597-2	2	13.59		19.46	
W597-3	2	16.46		19.73	

CELL ID	BOX#	EFF @ 1 SUN	EFF @ 125X	EFF @ 190X	GRID LINE %
W601-1	5	18.02		20.49	14.6
W601-3	5	16.83		20.18	16.6
W602-1	3	14.80		20.41	
W602-2	3	15.57		20.16	
W602-3	3	15.97		20.91	
W603-1	5	17.77		20.51	13.3
W603-2	3	17.12		20.29	
W603-3	5	15.79		20.31	17.7
W604-1	5	17.53		19.72	16.4
W604-2	6	16.23		19.68	11.8
W604-3	6	14.86		19.63	15.1
W605-1	1	17.77		20.46	
W605-2	5	17.11		20.57	16.1
W605-3	3	15.69		20.70	
W606-1	4	17.00		20.43	14.9
W606-2	4	13.83		20.41	13.6
W606-3	4	11.31			15.2
W607-1	1	17.85		20.54	
W607-2	1	17.03		20.71	
W607-3	4	13.19		20.19	16.2
W608-1	4	16.78		20.60	15.8
W608-2	5	17.33		20.87	14.5
W608-3	6	13.09		20.68	16.7

UNSW2

BARE-CELL DATA

CELL ID	BOX#	EFF @ 1 SUN	EFF @ 125X	EFF @ 190X	GRID LINE %
W616-1	6B	9.66		20.25	11.4
W616-2	6B	16.54		21.15	15.9
W616-3	6B	17.46		20.91	17.1
W627-1	6B	12.14		15.35	
W627-2	6T	15.64		17.63	
W627-3	6T	13.10		19.15	14.7
W628-1	6T	16.96		11.84	
W628-2	6T	11.08		11.70	
W628-3	6T	17.39		13.80	16.8
W631-1	3	18.49		21.43	14.5
W631-2	3	18.28		21.21	
W631-3	3	18.42		21.46	14.5
W632-1	3	18.59		20.01	
W632-2	3	18.81		20.40	12.1
W632-3	3	18.52		19.55	
W633-1	3	18.49		21.42	13.7
W633-2	2	18.87		21.58	13.4
W633-3	3	18.69		20.20	
W634-1	2	19.11		20.75	
W634-2	2	18.50		20.81	
W634-3	2	18.51		20.87	15.0
W635-1	2	18.38		21.18	
W635-2	2	18.72		21.20	12.0
W635-3	2	18.53		21.19	
W636-1	1	16.81		20.87	13.6
W636-2	1	18.30		19.50	
W636-3	2	18.45		20.61	
W637-1	1	18.51		19.35	
W637-2	1	18.35		20.45	
W637-3	1	18.42		20.84	14.8
W638-1	1	18.59		20.72	13.2
W638-2	1	18.47		20.17	
W638-3	1	18.09		20.37	

CELL ID	BOX#	EFF @ 1 SUN	EFF @ 125X	EFF @ 190X	GRID LINE %
W641-1	5B	17.90		20.96/	16.3
W641-2	5B	16.83		20.70	14.8
W641-3	5B	16.43		20.61/	17.1
W642-1	5B	16.51		19.50/	14.4
W642-2	5B	16.60		19.33/	16.5
W642-3	5B	16.18		19.13	
W643-1	5T	15.56		19.26	
W643-2	5T	16.35		19.38	
W643-3	5T	15.87		19.10	18.0
W644-1	5T	15.13		20.99	15.7
W644-2	4	18.29		21.04	
W644-3	5T	16.35		20.05	18.3
W645-1	4	17.81		20.87	
W645-2	4	17.46		20.54	
W645-3	4	17.64		20.31	
W646-1	4	16.41		20.47	
W646-2	4	15.12		21.16	
W646-3	4	17.03		20.24	
W648-1	4	17.87		21.22	
W648-2	4	15.46		20.82	
W648-3	4	16.81		20.42	
Z951-1	7B	17.96		20.52	16.1
Z951-2	7B	18.32		20.88	
Z951-3	7B	18.12		20.50	
Z953-1	7B	17.53		20.34	
Z953-2	7B	18.20		20.72	
Z953-3	7M	17.93		20.65	
Z956-1	7M	17.94		20.82	
Z956-2	7M	17.63		20.53	
Z956-3	7M	17.70		20.66	
Z957-1	7T	17.68		20.43	15.0
Z957-2	7T	17.30		20.26	
Z957-3	7T	17.11		20.00	

UNSW3
BARE-CELL DATA

CELL ID	BOX#	EFF @ 1 SUN	EFF @ 125X	EFF @ 190X	GRID LINE %
W471-1	3	18.54	21.67	21.53	14.2
W471-2	3	17.98	21.71	21.62	14.8
W471-3	3	17.50	22.00	21.81	11.6
W544-1	5	17.65	20.64	20.46	
W544-2	5	17.26	20.96	20.68	
W544-3	5	17.56	20.64	20.31	
W54C-1	5	17.84	21.03	20.94	
W54C-3	5	17.25	20.75	20.53	
W550-1	3	17.66	21.07	20.89	
W550-2	3	18.02	21.14	21.24	
W552-1	5	18.00	21.43	21.23	
W552-2	5	18.51	21.33	21.13	
W552-3	5	17.59	21.25	21.04	
W553-1	5	17.71	21.42	21.27	
W553-2	5	17.99	21.55	21.33	
W553-3	5	18.05	21.12	20.97	
W554-1	5	17.16	20.76	20.46	
W554-2	5	18.26	20.77	20.40	
W554-3	5	18.13	21.01	20.62	
W557-1	3	17.00	21.28	21.05	
W557-2	3	18.31	21.29	20.98	
W557-3	3	17.25	21.29	21.15	
W558-1	3	18.07	21.03	20.59	
W558-2	3	18.45	21.05	20.93	
W558-3	3	17.79	20.99	20.61	
W559-1	2	18.01	21.10	20.92	
W559-2	5	18.26	21.13	20.88	
W559-3	2	18.27	21.26	21.03	
W55C-2	3	19.12	22.01	21.72	13.0
W55C-3	3	18.46	21.68	21.50	14.6
W55D-1	3	17.78	21.36	21.07	
W55D-3	3	18.25	21.39	21.35	
Z793-1	1	16.70	19.15	18.03	
Z793-2	1	17.72	19.32	18.13	
Z793-3	1	17.10	19.54	18.61	
Z795-1	1	16.88	19.19	18.53	
Z795-2	4	18.07	19.41	18.64	
Z795-3	4	17.59	19.09	18.41	

CELL ID	BOX#	EFF @ 1 SUN	EFF @ 125X	EFF @ 190X	GRID LINE %
Z851-1	4	18.29	19.06	17.82	
Z851-3	4	17.07	18.48	17.35	
Z853-1	4	17.66	19.15	18.01	
Z853-2	4	18.35	17.71	15.99	
Z853-3	4	17.84	18.18	16.67	
Z855-1	2	18.11	21.24	21.00	
Z855-2	2	18.11	21.32	21.13	
Z855-3	2	17.65	20.68	20.50	
Z857-1	2	17.19	15.83	13.69	
Z857-2	2	17.49	16.06	13.82	
Z8510-1	4	18.13	21.04	20.75	
Z8510-2	2	18.11	21.29	20.85	
Z8510-3	2	18.08	21.03	20.69	
Z8512-1	4	18.61	20.61	19.83	
Z8512-2	4	17.98	19.93	19.33	
Z8512-3	4	17.80	20.27	19.67	
Z8513-1	1	17.71	20.81	20.39	
Z8513-2	1	18.27	20.97	20.75	
Z8521-1	4	17.77	20.26	19.42	
Z8521-2	4	18.48	19.85	19.10	
Z8521-3	4	17.90	20.24	19.72	
Z8525-1	1	17.57	21.04	20.90	
Z8525-2	1	17.98	21.32	21.16	
Z8525-3	1	17.78	21.06	20.98	
Z8528-1	2	17.78	21.04	20.98	
Z8528-2	2	17.97	21.21	21.11	
Z8528-3	2	18.14	21.30	21.18	
Z8529-1	1	17.69	20.94	20.84	
Z8529-2	1	17.82	21.01	20.90	
Z8529-3	1	17.49	21.26	21.05	
Z8531-1	1	18.24	21.16	21.03	
Z8531-2	1	18.42	21.60	21.23	
Z8531-3	1	17.87	21.10	20.93	
Z8532-1	2	18.06	21.27	21.08	
Z8532-2	2	18.37	21.28	21.01	
Z8532-3	2	17.91	21.06	20.89	
Z8533-2	4	15.65	20.36	19.89	
Z8533-3	4	17.11	20.47	19.79	

UNSW4
BARE-CELL DATA

CELL ID	BOX#	EFF @ 1 SUN	EFF @ 125X	EFF @ 190X	GRID LINE %
W611-1	BAD	12.72	21.95	21.62	
W611-2	2A5	18.02	21.72	21.48	
W611-3	2A5	16.51	21.71	21.37	
W651-1	BAD	16.59	19.78	19.78	
W651-2	BAD	15.85	19.12	19.04	
W651-3	BAD	15.34	18.84	18.81	
W652-1	2A5	17.69	20.13	19.60	
W652-2	BAD	16.21	19.52	18.98	
W652-3	2A5	17.36	19.83	19.50	
W653-1	2A5	17.31	19.98	19.60	
W653-2	2A4	17.30	19.99	19.62	
W653-3	BAD	16.42	19.16	18.84	
W654-1	BAD	16.92	19.06	18.43	
W654-2	BAD	16.88	17.96	16.95	
W654-3	BAD	16.28	18.62	18.13	
W656-1	BAD	13.13	16.90	16.40	
W656-2	BAD	14.56	17.16	16.81	
W656-3	BAD	14.32	17.54	17.50	
W658-1	2A4	17.58	18.92	17.93	
W658-2	BAD	16.39	18.85	18.41	
W658-3	BAD	16.08	18.25	17.80	
W662-1A	BAD	11.59	21.10	20.52	
W662-1?	BAD	16.47	21.33	21.30	
W662-1?	2A4	14.99	21.47	21.11	
W662-3	2A4	18.08	21.48	21.22	
W663-1	1/2	18.76	21.83	21.48	
W663-2	2A4	15.23	21.41	21.13	
W663-3	2A3	18.53	21.59	21.40	
W664-3	2A3	17.68	21.17	20.98	
W665-1	BAD	10.54	21.24	21.28	
W665-3	2A3	17.16	21.03	20.94	
W671-1	1/2	18.31	21.50	21.37	
W671-2	1/2	17.47	21.47	21.18	
W672-1	3	17.70	20.81	20.84	
W673-1	3	17.93	21.08	21.13	
W673-2	BAD	12.77	21.09	21.10	
W675-1	2B3	14.76	21.44	21.23	
W675-2	2B3	14.84	21.36	21.25	
W675-3	BAD	10.53	21.19	21.10	
W676-1	1/2	18.23	21.36	21.08	
W676-2	4	13.40	21.67	21.58	
W676-3	1/2	17.07	21.49	21.38	
W681-1	3	18.48	21.75	21.46	
W681-2	3	17.48	21.89	21.76	
W681-3	3	18.35	21.53	21.31	
W682-1	3	18.17	22.02	21.77	
W682-2	3	19.31	22.05	21.58	
W682-3	3	18.72	22.01	21.76	
W683-1	3	18.95	21.91	21.65	
W683-2	3	18.25	22.01	21.86	
W683-3	3	18.54	21.91	21.74	
W684-1	3	18.88	21.71	21.60	
W684-2	3	18.12	21.83	21.56	
W684-3	3	18.53	21.70	21.61	
W685-1	3	17.90	21.88	21.60	
W685-2	3	18.49	21.58	21.46	
W685-3	3	17.51	21.69	21.49	
W686-1	3	18.94	21.69	21.32	
W686-2	3	18.91	21.53	20.90	
W686-3	3	18.61	21.58	21.18	
Z906-1	2B2	14.04	21.25	20.90	
Z906-2	2B2	17.18	21.51	21.19	
Z906-3	2B2	16.35	21.09	20.79	
Z907-1	2B2	17.30	21.48	21.23	
Z907-2	7/6	16.05	21.59	21.46	
Z907-3W	7/7	16.99	21.02	20.95	
Z933-1	5	17.65	19.29	18.20	
Z933-2	4	17.07	19.83	18.95	
Z933-3	5	17.63	19.10	18.25	
Z937-1	4	17.82	21.27	21.12	
Z937-2	4	10.95	21.46	21.21	
Z937-3	4	14.70	20.78	20.49	

UNSW4 (CONTINUED)
BARE-CELL DATA

CELL ID	BOX#	EFF @ 1 SUN	EFF @ 125X	EFF @ 190X	GRID LINE %
Z940-1	4	17.74	20.78	20.24	
Z944-1	4	17.54	20.50	20.26	
Z960-1	1B	17.80	20.55	20.27	
Z960-2	1B	17.61	20.55	20.25	
Z960-3	1B	17.65	20.66	20.34	
Z962-1	5	17.47	20.34	19.77	
Z962-2	5	16.82	19.92		
Z962-3	5	17.09	19.90	19.63	
Z963-1	1B	17.70	20.54	20.21	
Z963-2	7	17.17	20.25	19.90	
Z963-3	7	16.93	19.85	19.47	
Z965-1	1B	17.75	20.52	20.15	
Z965-2	1B	17.95	20.71	20.27	
Z965-3	2B2	17.56	20.56	20.40	
Z966-1	1B	17.77	20.97	20.47	
Z966-2	1B	17.52	20.66	20.36	
Z966-3	2B1	17.04	20.21	20.05	
Z967-1	1A	16.17	20.76	20.64	
Z967-2	1A	17.40	20.52	20.18	
Z967-3	1A	16.76	20.09	19.93	
Z969-1	1A	18.12	21.20	20.82	
Z969-2	1A	17.86	21.17	20.92	
Z969-3	1A	17.65	20.89	20.69	
Z1000-1	7	16.64	19.78	19.50	
Z1000-2	7	16.49	19.43	19.06	
Z1000-3W	7/6	16.14	19.08	18.93	
Z1001-1	SAR	13.72	20.17	19.66	
Z1001-2	SAR	17.71	20.31	19.69	
Z1001-3	SAR	17.12	20.05	19.49	
Z1002-1	2B1	17.58	20.63	20.21	
Z1002-2	2B1	17.51	20.79	20.47	
Z1002-3	2B1	17.53	20.38	20.13	
Z1003-1	7	17.66	20.36	19.77	
Z1003-2	7	17.75	20.52	19.83	
Z1003-3	3	17.45	20.21	19.83	
Z1004-1	7	17.94	20.96	20.67	
Z1004-2	7	17.29	20.95	20.54	
Z1004-3	7	17.86	20.82	20.50	
Z1005-1	3	17.19	20.70	20.23	
Z1005-2	2B1	17.40	20.58	20.20	
Z1005-3	2B1	17.87	20.71	20.37	
Z1006-1	1A	17.91	20.56	19.54	
Z1006-2	1A	18.52	20.54	19.78	
Z1006-3	1A	18.43	20.48	19.76	
Z1007-1	1A	17.41	20.50	20.13	
Z1007-2	1A	17.18	20.20	19.70	
Z1007-3	1A	17.28	20.30		
Z1008-1	NAR	15.77	18.54	18.32	
Z1008-2	NAR	13.74	18.00	17.72	
Z1008-3	NAR	14.71	17.96	17.78	
Z1012-1	3	17.59	14.24	12.34	
Z1012-2	3	17.70	13.76	11.51	
Z1012-3	3	17.51	11.04	8.90	
Z1014-1	6	17.96	17.95	16.07	
Z1014-2	6	16.91	13.86	11.67	
Z1014-3	6	16.74	10.76	8.78	
Z1015-1	6	17.22	20.40	20.12	
Z1015-2	6	16.61	18.17	16.80	
Z1015-3	6	17.35	17.11	15.74	
Z1016-1	6	16.49	19.13	18.12	
Z1016-2	5	16.49	13.29	11.26	
Z1016-3	5	14.16	13.69	11.69	
Z1017-1	SAR	17.83	14.75	12.48	
Z1017-2	SAR	17.80	12.83	10.71	
Z1017-3	SAR	16.74	11.19	8.81	
Z1018-1	NAR	15.29	12.26	10.66	
Z1018-2	NAR	14.77	15.16	13.94	
Z1018-3	NAR	15.20	14.40	13.11	

UNSW5

BARE-CELL DATA

CELL ID	BOX#	EFF @ 1 SUN	EFF @ 125X	EFF @ 190X	GRID LINE %
W000	4	15.55	20.63	20.25	
W690-1	4	10.58	18.90	18.75	
W690-2	4	14.20	19.32	19.12	
W690-3	4	14.66	19.21	18.76	
W691-1	5	16.77	19.69	19.52	
W691-2	5	16.92	19.65	19.25	
W691-3	5	16.60	19.30	19.03	
W692-1	5	16.61	19.80	19.48	
W692-2	5	15.05	20.39	20.17	
W692-3	5	16.70	19.63	19.48	
W694-1	5	16.10	18.92	18.83	
W694-2	5	16.02	18.98	18.80	
W694-3	5	16.07	19.04	18.84	
W695-1	5	18.37	21.28	20.97	
W695-2	5	18.43	21.33	21.14	
W695-3	5	18.31	21.13	20.79	
W696-1	1	18.83	21.95	21.86	
W696-2	1	18.50	21.97	21.75	
W696-3	1	18.62	21.79	21.65	
W697-1	1	19.02	21.92	21.58	
W697-2	1	18.99	21.91	21.55	
W697-3	1	18.70	21.50	21.21	
W698-1	1	18.98	21.79	21.56	
W698-2	1	18.94	21.92	21.65	
W698-3	1	18.41	21.76	21.56	
W699-1	1	18.43	21.13	20.90	
W699-2	1	17.46	21.24	20.86	
W699-3	1	18.56	21.16	20.82	
W69A-1	3	17.65	20.64	20.38	
W69A-2	3	17.60	21.14	20.80	
W69A-3	3	16.90	20.69	20.21	
W69B-1	3	17.36	18.99	18.13	
W69B-2	3	17.38	19.67	18.87	
W69B-3	4	16.71	18.46	16.93	
W69C-1	4	15.97	20.00	19.97	
W69C-2	4	13.50	19.38	18.82	
W69C-3	4	14.94	19.76	19.58	

CELL ID	BOX#	EFF @ 1 SUN	EFF @ 125X	EFF @ 190X	GRID LINE %
W69E-1	4	15.43	16.50	15.30	
W69E-2	4	15.40	17.25	16.16	
W69E-3	4	13.18	16.52	15.46	
W69F-2	4	15.04	10.44	9.27	
W69F-3	4	14.73	11.23	9.94	
W700-1	2	18.79	21.62	21.35	
W700-2	2	18.56	21.34	21.07	
W700-3	2	18.26	21.12	20.90	
W701-1	2	17.75	21.41	21.17	
W701-2	2	17.60	21.27	21.10	
W701-3	2	15.44	20.89	20.80	
W703-1	3	18.94	22.20	22.11	
W703-2	2	18.79	21.92	21.83	
W703-3	2	18.37	21.38	21.22	
W704-1	2	18.77	21.85	21.72	
W704-2	2	18.90	21.95	21.77	
W704-3	2	18.44	21.48	21.39	
W705-1	5	18.63	21.43	21.25	
W705-2	5	18.54	21.49	21.24	
W705-3	5	17.85	20.77	20.63	
W706-1	2	16.78	20.87	20.50	
W706-2	2	16.95	20.84	20.54	
W706-3	2	15.52	20.62	20.36	
W707-1	5	16.61	20.08	19.76	
W707-2	5	16.60	20.40	20.05	
W707-3	5	15.30	19.80	19.45	
W708-1	4	15.03	20.36	20.12	
W708-2	4	16.61	20.22	19.66	
W708-3	4	15.51	20.34	20.11	
W709-1	3	18.86	21.97	21.65	
W709-2	3	18.86	21.79	21.26	
W709-3	3	18.52	21.60	21.38	
W711-1	3	18.51	21.66	21.28	
W711-2	1	18.27	21.05	20.66	
W711-3	3	18.19	21.26	21.02	

UNSW5 (CONTINUED)
BARE-CELL DATA

CELL ID	BOX#	EFF @ 1 SUN	EFF @ 125X	EFF @ 190X	GRID LINE %
W712-1	4	16.49	20.52	20.25	
W712-2	4	16.24	20.24	19.94	
W712-3	4	15.57	19.97	19.67	
W713-1	3	17.34	21.25	20.93	
W713-2	3	18.11	21.25	20.81	
W713-3	3	17.97	20.88	20.62	
W715-1	4	16.11	20.15	20.18	
W715-2	4	15.30	19.45	19.17	
W715-3	4	14.23	19.59	19.60	

CELL ID	BOX#	EFF @ 1 SUN	EFF @ 125X	EFF @ 190X	GRID LINE %
W716-1	4	13.49	19.92	19.83	
W716-2	4	15.35	19.63	19.43	
W716-3	4	13.78	19.28	19.24	
W717-1	4	16.62	20.36	20.38	
W717-2	4	20.73	20.55	20.16	
W717-3	4	16.11	20.65	20.37	
W718-1	4	15.72	19.88	19.74	
W718-2	4	15.02	19.29	19.09	
W718-3	4	13.83	19.23	19.04	

APPENDIX C

SANDIA MEASUREMENT SUMMARY AFTER SOLDERING & APPLICATION OF PRISMATIC COVERS

CELL PERFORMANCE AFTER SOLDERING AND APPLICATION OF PRISMATIC COVERS

CELL ID	BOX#	EFF @ 1 SUN	EFF @ 125X	EFF @ 190X	GRID LINE %	EFF* OF CELL AS	EFF** OF CELL AS	EFF* W/ PRISM C	EFF** W/ PRISM C
UNSW1 W574-2	6	15.86		18.85	~17?		19.22		22.46
UNSW1 W574-3	1	16.81		18.64	~17?		18.73		21.85
UNSW1 W575-1	6	13.85		18.85	17.2		19.17	22.09	21.27
UNSW1 W575-2	6	16.42		19.47	16.0		19.64	22.92	22.36
UNSW1 W594-1	4	13.55		20.45	14.0		20.60	24.30	23.96
UNSW1 W601-1	5	18.02		20.49	14.6		20.34	23.08	22.80
UNSW1 W601-3	5	16.83		20.18	16.6		20.02	23.59	23.34
UNSW1 W603-1	5	17.77		20.51	13.3		20.24	23.30	22.88
UNSW1 W603-3	5	15.79		20.31	17.7		20.13	23.25	23.01
UNSW1 W604-1	5	17.53		19.72	16.4		19.55	22.46	21.99
UNSW1 W604-2	6	16.23		19.68	11.8		19.43	22.46	21.69
UNSW1 W604-3	6	14.86		19.63	15.1		19.50	22.30	21.85
UNSW1 W605-2	5	17.11		20.57	16.1		20.33	22.79	22.62
UNSW1 W606-1	4	17.00		20.43	14.9		20.31	24.00	23.63
UNSW1 W606-2	4	13.83		20.41	13.6		20.46	22.99	22.73
UNSW1 W606-3	4	11.31			15.2		20.02	22.97	22.91
UNSW1 W607-3	4	13.19		20.19	16.2		20.12	23.21	23.09
UNSW1 W608-1	4	16.78		20.60	15.8		20.65	23.62	23.44
UNSW1 W608-2	5	17.33		20.87	14.5		20.66	23.59	23.32
UNSW1 W608-3	6	13.09		20.68	16.7		20.77	23.22	23.09
UNSW2 W616-1	6B	9.66		20.25	11.4	20.70	20.56		
UNSW2 W616-3	6B	17.46		20.91	17.1			24.63	24.57
UNSW2 W627-3	6T	13.10		19.15	14.7	19.48	18.65	22.36	21.45
UNSW2 W631-1	3	18.49		21.43	14.5	21.51	21.34	23.70	
UNSW2 W631-3	3	18.42		21.46	14.5	20.93	20.57	23.54	23.21
UNSW2 W632-2	3	18.81		20.40	12.1	21.04	20.38	23.00	22.32
UNSW2 W633-1	3	18.49		21.42	13.7	21.56	21.17	24.14	23.76
UNSW2 W633-2	2	18.87		21.58	13.4	21.51	21.28	24.09	23.73
UNSW2 W634-3	2	18.51		20.87	15.0	21.07	20.65	23.98	23.57
UNSW2 W635-2	2	18.72		21.20	12.0	21.89	21.41	23.99	23.50
UNSW2 W636-1	1	16.81		20.87	13.6	21.29	20.94	23.74	23.35
UNSW2 W637-3	1	18.42		20.84	14.8	21.35	20.97	23.94	23.50
UNSW2 W638-1	1	18.59		20.72	13.2	21.10	20.48		23.00
UNSW2 W641-1	5B	17.90		20.96	16.3	21.04	20.79	23.52	23.34
UNSW2 W641-2	5B	16.83		20.70	14.8	20.93	20.66	23.34	23.15
UNSW2 W641-3	5B	16.43		20.61	17.1	20.73	20.47		
UNSW2 W642-1	5B	16.51		19.50	14.4	19.39	19.00	22.12	21.91
UNSW2 W643-3	5T	15.87		19.10	18.0	19.11	18.94	22.43	22.26
UNSW2 Z951-1	7B	17.96		20.52	16.1	21.07	20.83	24.45	24.10
UNSW3 W471-1	3	18.54	21.67	21.53	14.2	21.69	21.39	24.45	24.16
UNSW3 W471-2	3	17.98	21.71	21.62	14.8	21.89	21.57	25.04	24.82
UNSW3 W471-3	3	17.50	22.00	21.81	11.6	22.01	21.43	24.56	24.15
UNSW3 W55C-2	3	19.12	22.01	21.72	13.0	21.73	21.17	24.20	23.79
UNSW3 W55C-3	3	18.46	21.68	21.50	14.6	21.50	20.99	24.15	23.73

*EFFICIENCY MEASURED AT 125X
**EFFICIENCY MEASURED AT 190X
NO CORRECTIONS FOR SPECTRAL MISMATCH

DO NOT MICROFILM
THIS PAGE

DISTRIBUTION LIST

Acrian (2)
Attn: Mary Bernstein
Bill Ruehle
490 Race Street
San Jose, CA 95126

AESI, Inc.
Attn: William J. Todorof
1001 W. 17th Street, Unit V
Costa Mesa, CA 92627

Alpha Solarco (2)
Attn: Edward Schmidt
Don Carroll
11534 Gondola Dr.
Cincinnati, OH 45241

Amonix, Inc.
Attn: Vahan Garboushian
3545 W. Lomita Blvd
Unit A
Torrance, CA 90505

American Optical Corporation (2)
Attn: Clark Grendol
R. F. Woodcock
14 Mechanic Street
Southbridge, MA 01550

Applied Solar Energy Corp (3)
Attn: Charlie Chu
Dave Kozak
Ken Ling
15251 E. Don Julian Road
City of Industry, CA 91746

ARCO Solar, Inc. (2)
Attn: Charles Gay
Kim Mitchell
P. O. Box 6032
Camarillo, CA 93010

Arizona Public Service Company
Attn: Tom Lepley
P. O. Box 53999
Mail Station 9110
Phoenix, AZ 85072-3999

Arizona State University (2)
College of Engineering and Applied Science
Attn: Charles Backus
G. H. Schwuttke
Tempe, AZ 85287

Astropower Division (2)
Attn: A. Barnett
R. Hall
30 Lovett Avenue
Newark, DE 19711

Bechtel National, Inc.
Attn: Walter J. Stolte
Mail Stop 50/15/D17
P. O. Box 3965
San Francisco, CA 94119

Black & Veatch
Attn: Sheldon L. Levy
P. O. Box 8405
11401 Lamar
Kansas City, MO 64114

Boeing Electronics Company
Attn: Lewis Fraas
P. O. Box 24969, MS 9Z-80
Seattle, WA 98124-6269

California Institute of Technology
Electrical Engineering Dept.
Attn: Marc A. Nicolet
116-81
Pasadena, CA 91125

City of Austin
Electric Dept.
Attn: John E. Hoffner
P. O. Box 1088
Austin, TX 78767

Electric Power Research Inst. (2)
Attn: Frank Goodman
Ed DeMeo
3412 Hillview Avenue
P. O. Box 10412
Palo Alto, CA 94303

ENTECH (2)
Attn: Walter Hess
Mark O'Neill
P. O. Box 612246
DFW Airport, TX 75261

Max Findel
836 Rio Arriba Avenue, SE
Albuquerque, NM 87123

Fresnel Optics, Inc.
Attn: John Egger
1300 Mt. Read Blvd.
Rochester, NY 14606

General Dynamics/Space Systems
Attn: Ted Stearn
Mail Zone 24-8730
P. O. Box 85990
San Diego, CA 92138

Georgia Institute of Technology
School of Electrical Engineering
Attn: Professor Ajeet Rohatgi
Atlanta, GA 30332

Heliopower, Inc.
Attn: Joel Davidson
P. O. Box 5089
Culver City, CA 90231

High Intensity Photovoltaics, Inc.
Attn: Bernard L. Sater
9007 Westlawn Blvd.
Olmsted Falls, OH 44138

Hughes Research Labs (2)
Attn: S. Kamath
Robert Loo
3011 Malibu Canyon Road
Malibu, CA 90265

James Associates
Attn: Larry James
1525 E. County Road 58
Fort Collins, CO 80524

Jet Propulsion Laboratory (2)
Attn: Ron Ross
R. S. Sugimura
4800 Oak Grove Drive
Pasadena, CA 91109

Kopin Corporation
Attn: Mark Spitzer
695 Myles Standish Blvd.
Taunton, MA 02780

Luz Engineering Corp.
Attn: David Kearny
924 Westwood Blvd., Suite 1000
Los Angeles, CA 90024

MIT/Lincoln Lab
Attn: George Turner
Box 73
Lexington, MA 02173

Mobil Solar Energy Corporation
Attn: Juris Kalejs
4 Suburban Park Drive
Billerica, MA 01821

New Mexico State University (2)
Attn: L. Matthews
G. Mulholland
P. O. Box 3450
Las Cruces, NM 88003

NYSERDA
Attn: Burton Krakow
2 Rockefellar Plaza
Albany, NY 12223

Ohio State University
Welding Department
Attn: Charles Albright
190 West 19th Street
Columbus, OH 43210

Pacific Gas & Electric (2)
Attn: Steve Hester
Mary Ilyin
3400 Crow Canyon Road
San Ramon, CA 94583

Public Service Company
of New Mexico
Attn: R. Frank Burcham
Alvarado Square, MS 0150
Albuquerque, NM 87158

Purdue University
Attn: Richard Schwartz
School of Electrical Engineering
West Lafayette, IN 47907

SAIC
Attn: Kelly Beninga
10343 Roselle St., Suite G
San Diego, CA 92121

SEA Corp.
Attn: Donald Curchod
2010 Fortune Dr., Suite 102
San Jose, CA 95131

SERA Solar Corporation
Attn: James Gibbons
3151 Jay Street
Santa Clara, CA 95054

SERI (4)
Attn: John Benner
Bushan Sopori
Tom Surek
E. Witt
1617 Cole Blvd.
Golden, CO 80401

SERI Library
1617 Cole Blvd.
Golden, CO 80401

Solarex Aerospace Division (2)
Attn: Jerry Silver
Ramon Dominguez
201 Perry Parkway, Suite 1
Gaithersburg, MD 20877

Solarex Corporation
Attn: John Wohlgemuth
630 Solarex Court
Frederick, MD 21701

Solar Kinetics Inc.
Attn: Gus Hutchinson
10635 King William Dr.
Dallas, TX 75220

SOLEC International, Inc.
Attn: Ishaq Shahryar
12533 Chadron Avenue
Hawthorne, CA 90250

Southern California Edison
Attn: Nick Patapoff
2244 Walnut Grove Avenue
Rosemead, CA 91770

Sparta
Attn: Ugur Ortabasi
5673 W. Las Positas Blvd.
Suite 205
Pleasonton, CA 94566

SPECO
Attn: Walt Hart
P. O. Box 91
Morrison, CO 80465

Spectrolab
Attn: David Lillington
12500 Gladstone Avenue
Sylmar, CA 91342

Spire Corporation (2)
Attn: M. J. Nowlan
Steve Tobin
Patriots Park
Bedford, MA 01730

Stanford University (2)
Attn: Richard Swanson
Ron Sinton
McCullough 206
Stanford, CA 94305

Tactical Fabs, Inc.
Attn: Richard Bechtel
270 East Brokaw Rd.
San Jose, CA 95112

3M Company (3)
Solar Optical Products
Attn: Sanford Cobb, 235-BC-05
Paul Jaster, 225-2N-06
Al Zderad, 235, BC-05
3M Center
St. Paul, MN 55144

U. S. Department of Energy
Albuquerque, Operations Office
Attn: George Tennyson
P. O. Box 5400
Albuquerque, NM 87115

U. S. Department of Energy (9)
Attn: Robert Annan
Morton Prince
Andrew Krantz
Lloyd Herwig (5)
Richard King
1000 Independence Avenue, SW
Washington, DC 20585

University of Arizona
Solar & Energy Research Facility
Attn: D. E. Osborn
CE Bldg. #76
Tucson, AZ 85721

University of Chicago
Attn: Joseph O'Gallagher
5640 South Ellis Avenue
Chicago, IL 60637

University of New Mexico/NMERI
Attn: G. Leigh
Campus Box 25
Albuquerque, NM 87131

University of New South Wales (5)
Department of Electrical Engr.
Attn: Martin A. Green
P. O. Box 1
Kensington, New South Wales
Australia 2003

Varian Associates
Attn: G. Virshup
611 Hansen Way, MS K-124
Palo Alto, CA 94303

Wattsun
Attn: John Doherty
P. O. Box 751
Albuquerque, NM 87103

Westinghouse Electric Corporation
Attn: Charles Rose
P. O. Box 10864
Pittsburgh, PA 15236

Wright Patterson AFB
Attn: Jack Geis
AFWAL/POOC
Wright Patterson AFB, OH

1890	R. G. Kepler
1812	C. L. Renschler
1811	L. Salgado
1812	R. A. Assink
1820	J. B. Woodard
1830	M. J. Davis
1840	R. E. Loehman
6000	D. L. Hartley
6200	V. L. Dugan
6220	D. G. Schueler
6221	E. C. Boes
6221	J. E. Cannon
6221	J. L. Chamberlin
6221	C. J. Chiang
6221	A. B. Maish (10)
6221	C. B. Stillwell
6223	G. J. Jones
6224	D. E. Hasti
6224	D. L. King (5)
8524	J. A. Wackerly
3141	S. A. Landenberger (5)
3141-1	C. L Ward For DOE/OSTI (8)
3151	W. I. Klein (3)